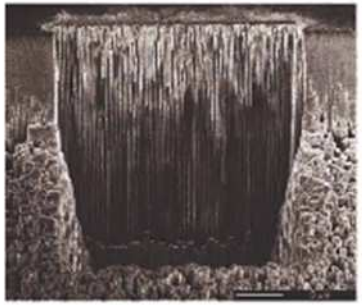
Figure 1. Nanoproteomics for personalized medicine

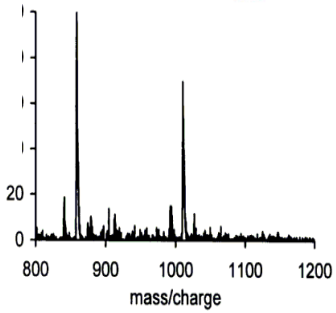


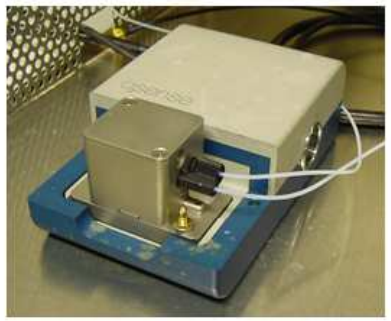
Human blood, urine, saliva and other samples



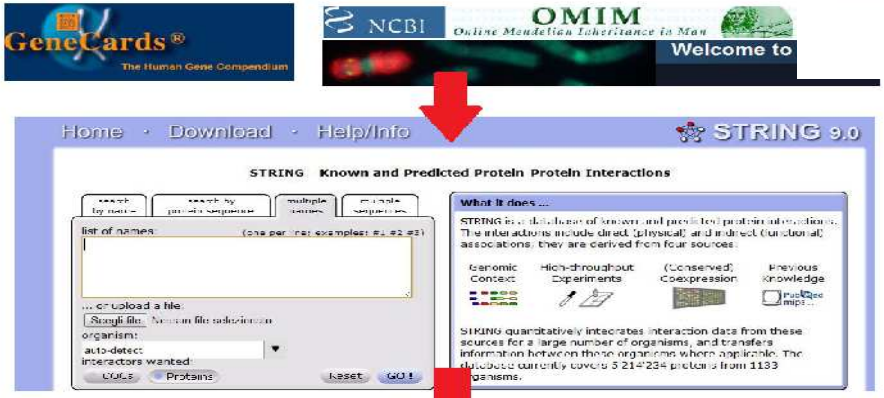


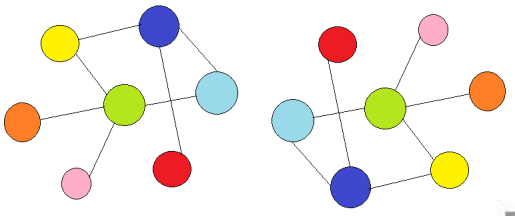






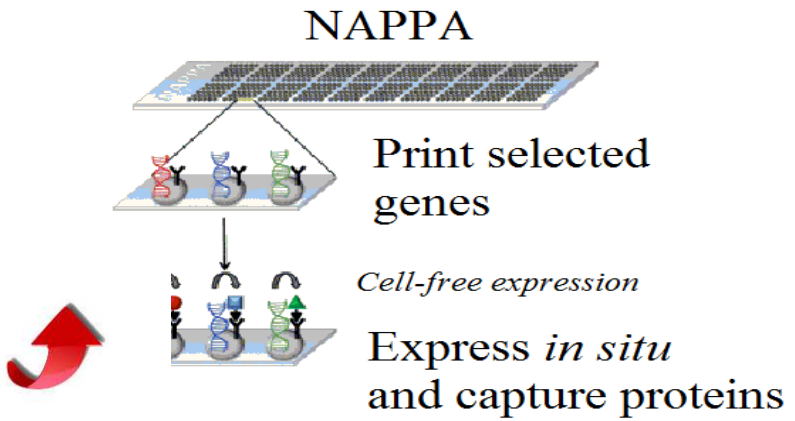
Identification of highly interacting genes

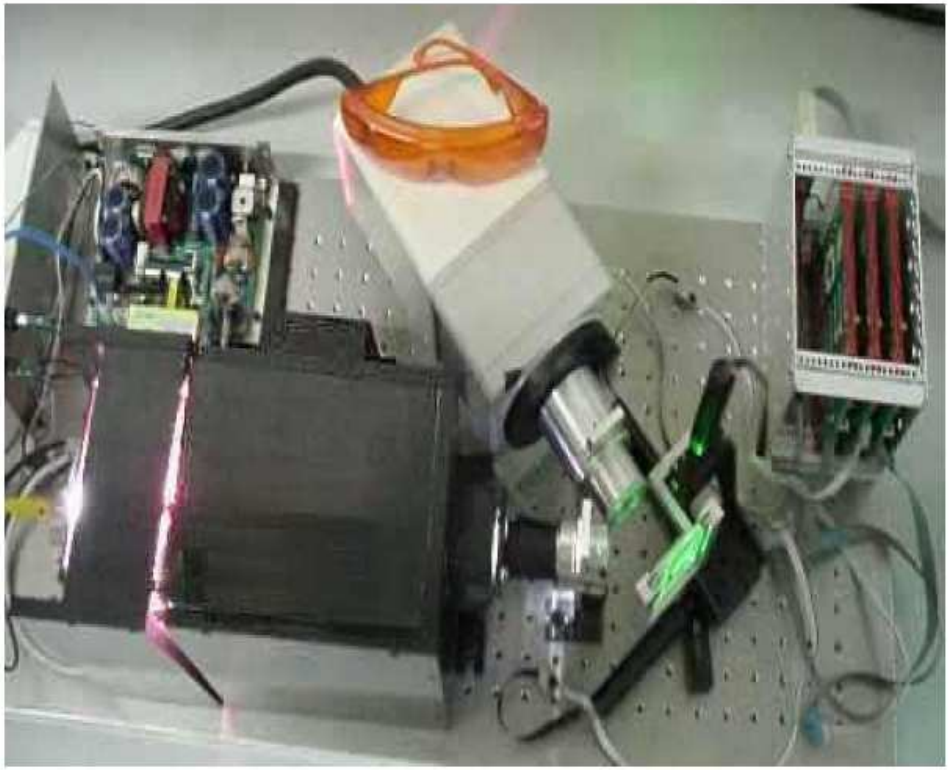


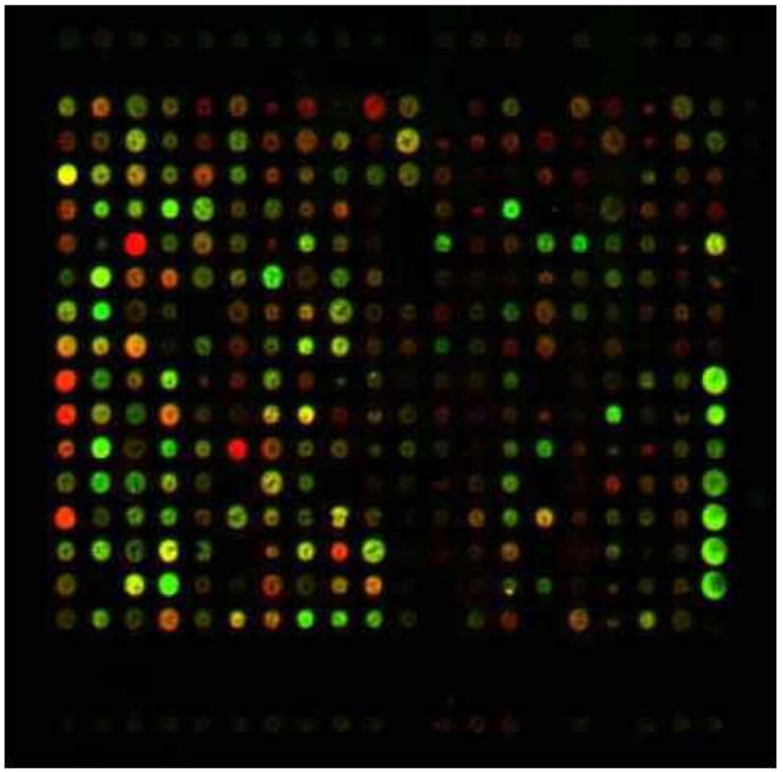




Label-free nanobiotechnologies (APA ,QMC_D and Mass Spectrometry)







DNASER

DNA Chip Matrix

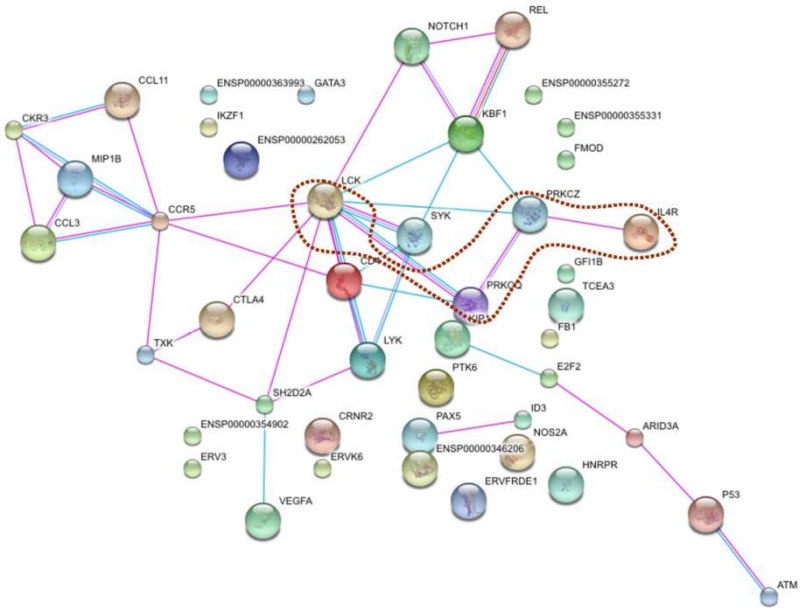


Figure 2 Indentification of leading genes by bioinformatics (below) and DNASER for fluorescence analysis (left, above) of genes microarray (right, above). Interaction network for genes distinguishing lymphoma from normal T cells. Subnetwork connecting the four leader genes which are “neutral” according to their expression pattern are shown with a dotted line.

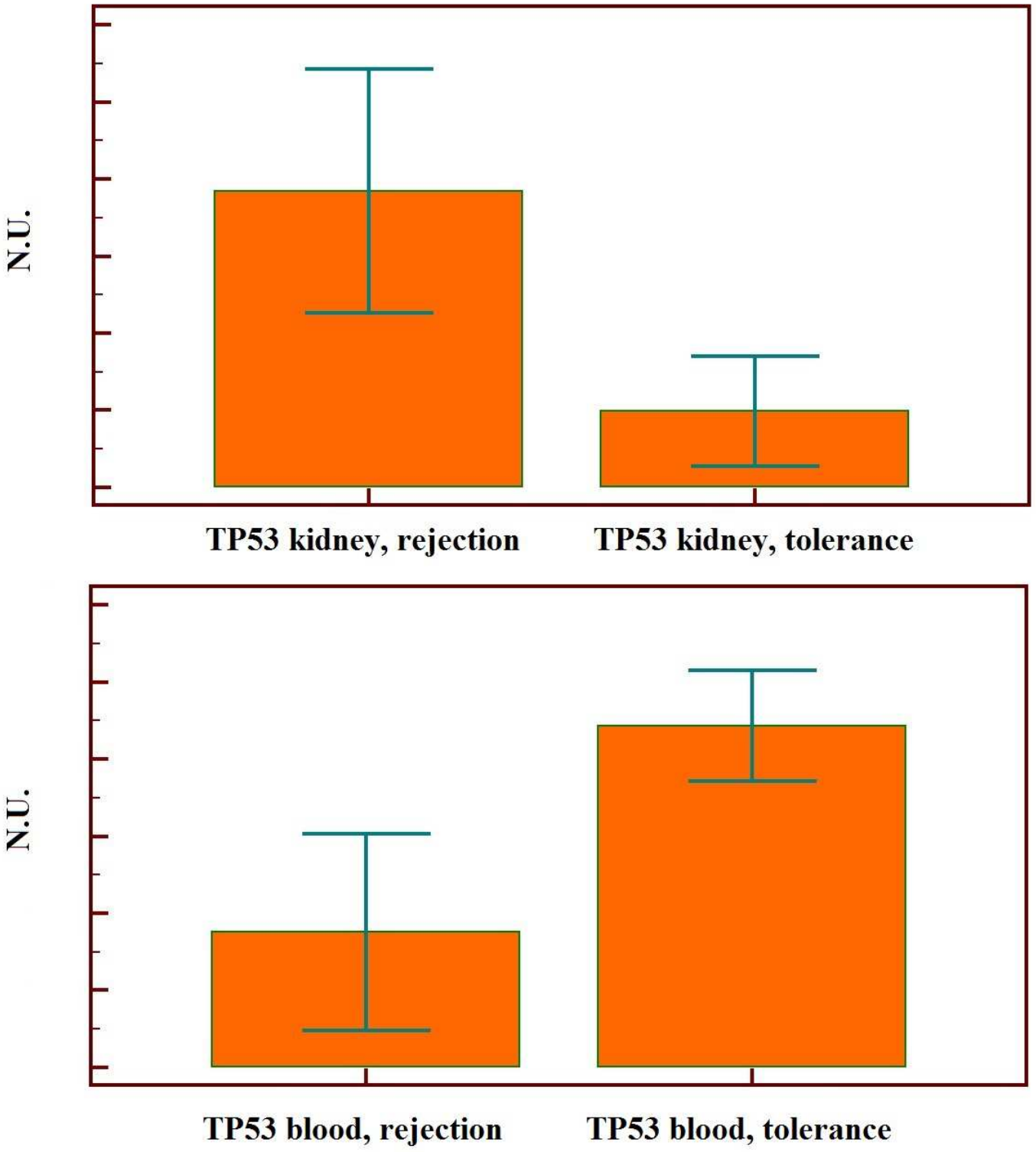
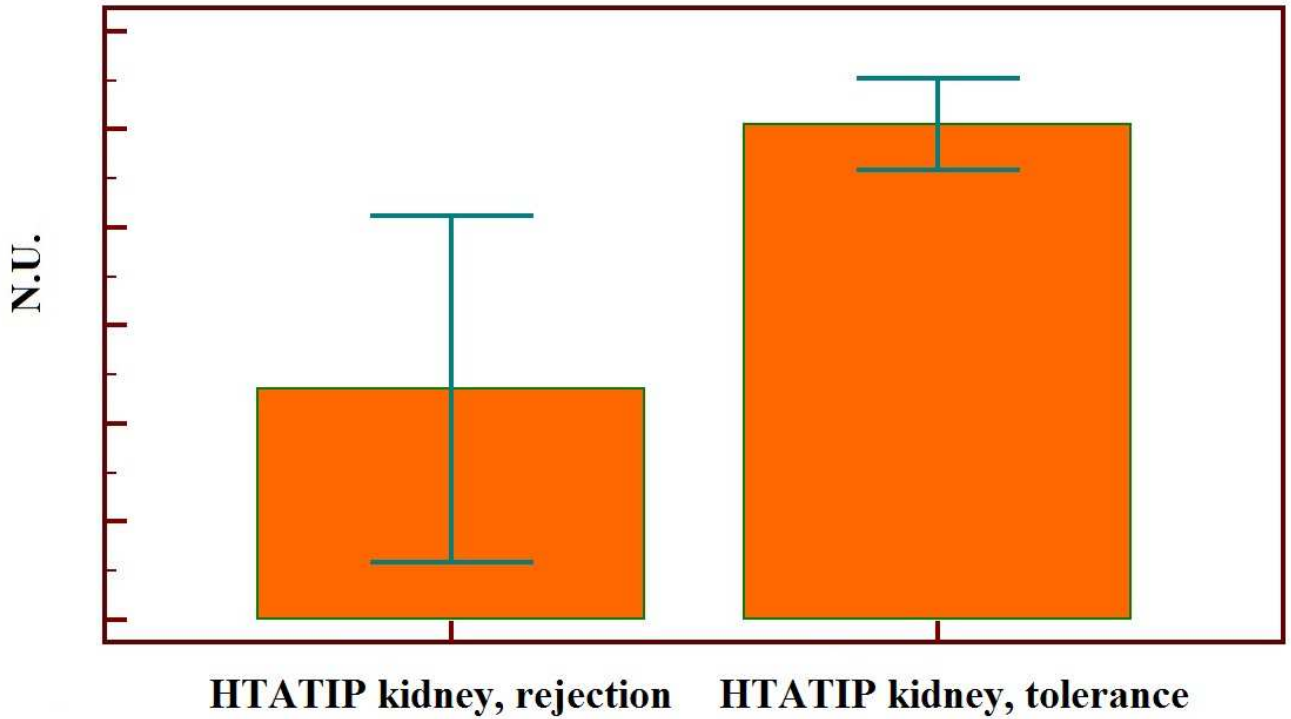


Figure 1. TP53 profile expression, which is differentially expressed between tolerant patients and those who have rejected renal graft. It is a predictor both in kidney and in peripheral blood.



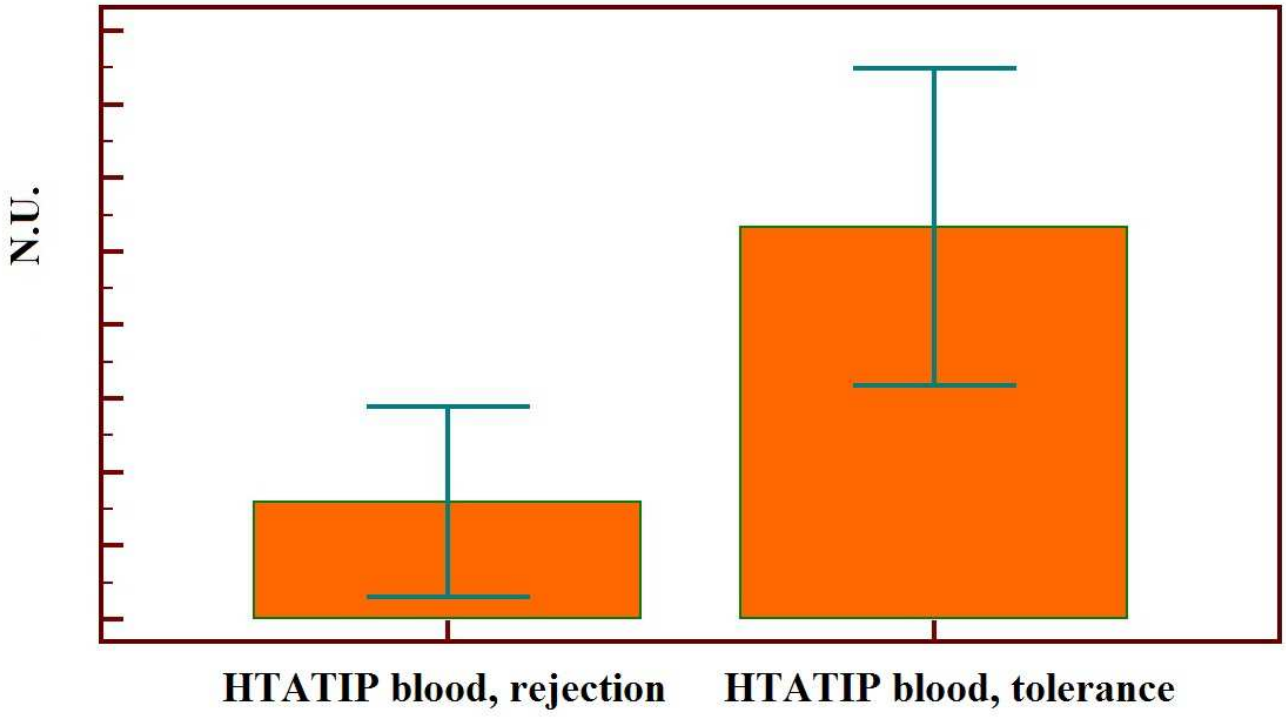
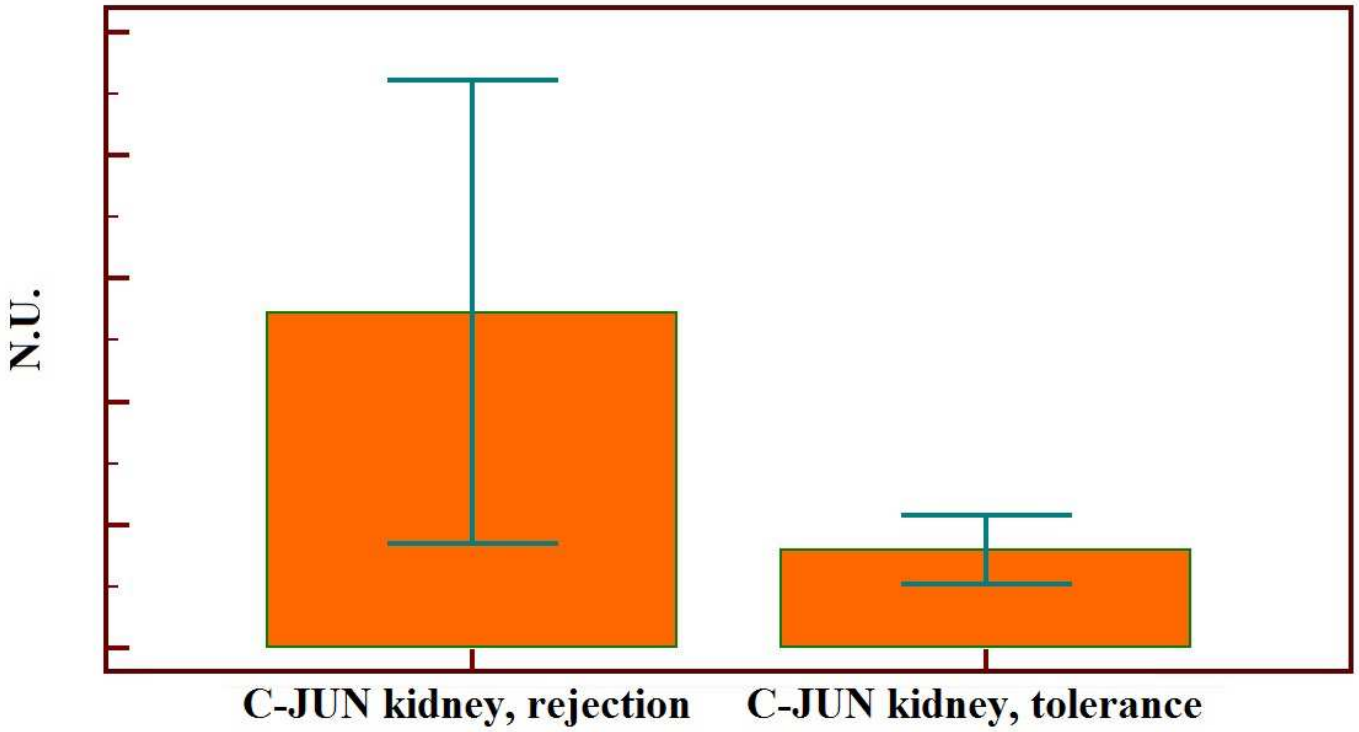


Figure 2. HTATIP profile expression, which is differentially expressed between tolerant patients and those who have rejected renal graft. It is a predictor both in kidney and in peripheral blood.



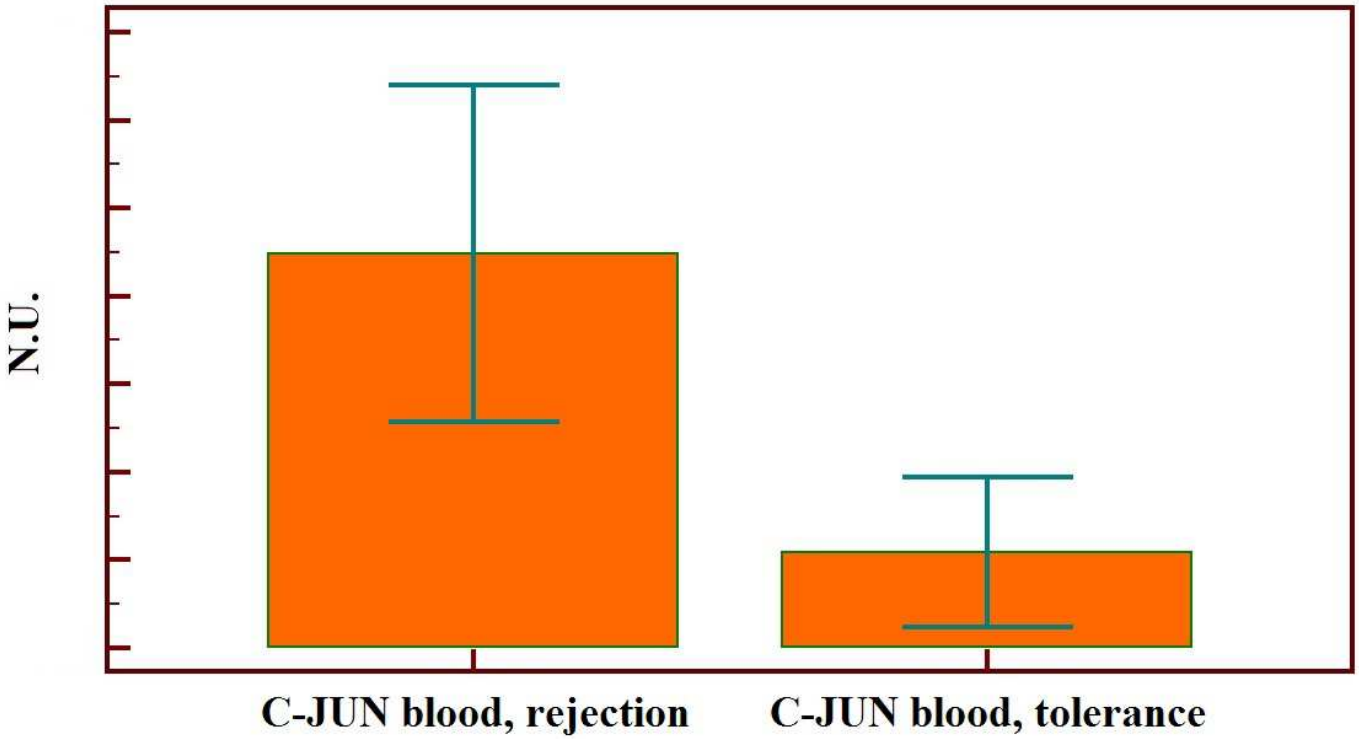


Figure 3. C-JUN profile expression, which is differentially expressed between tolerant patients and those who have rejected renal graft. It is a predictor both in kidney and in peripheral blood.

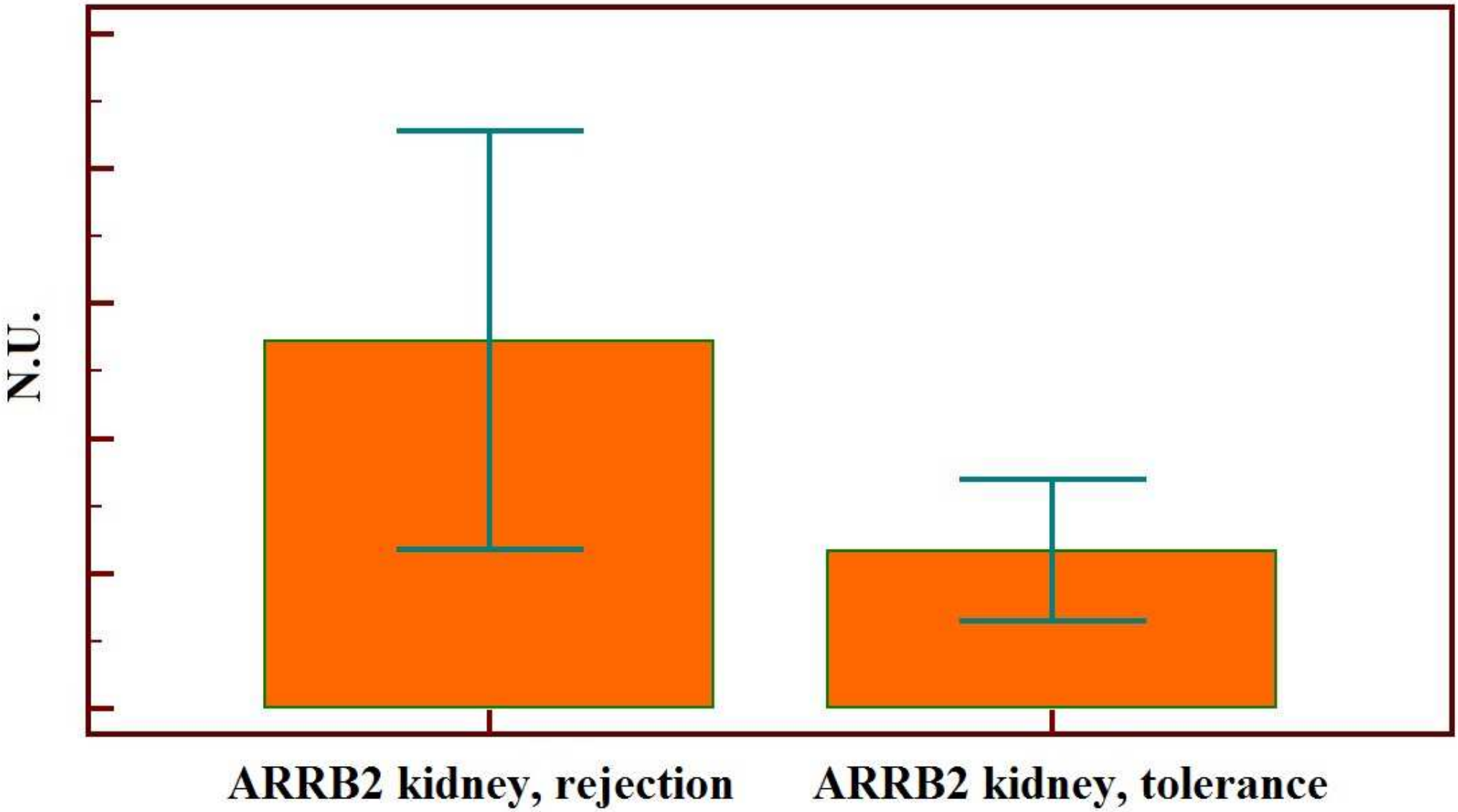


Figure 4. ARRB2 profile expression, which is differentially expressed between tolerant patients and those who have rejected renal graft. It is a predictor only in kidney.

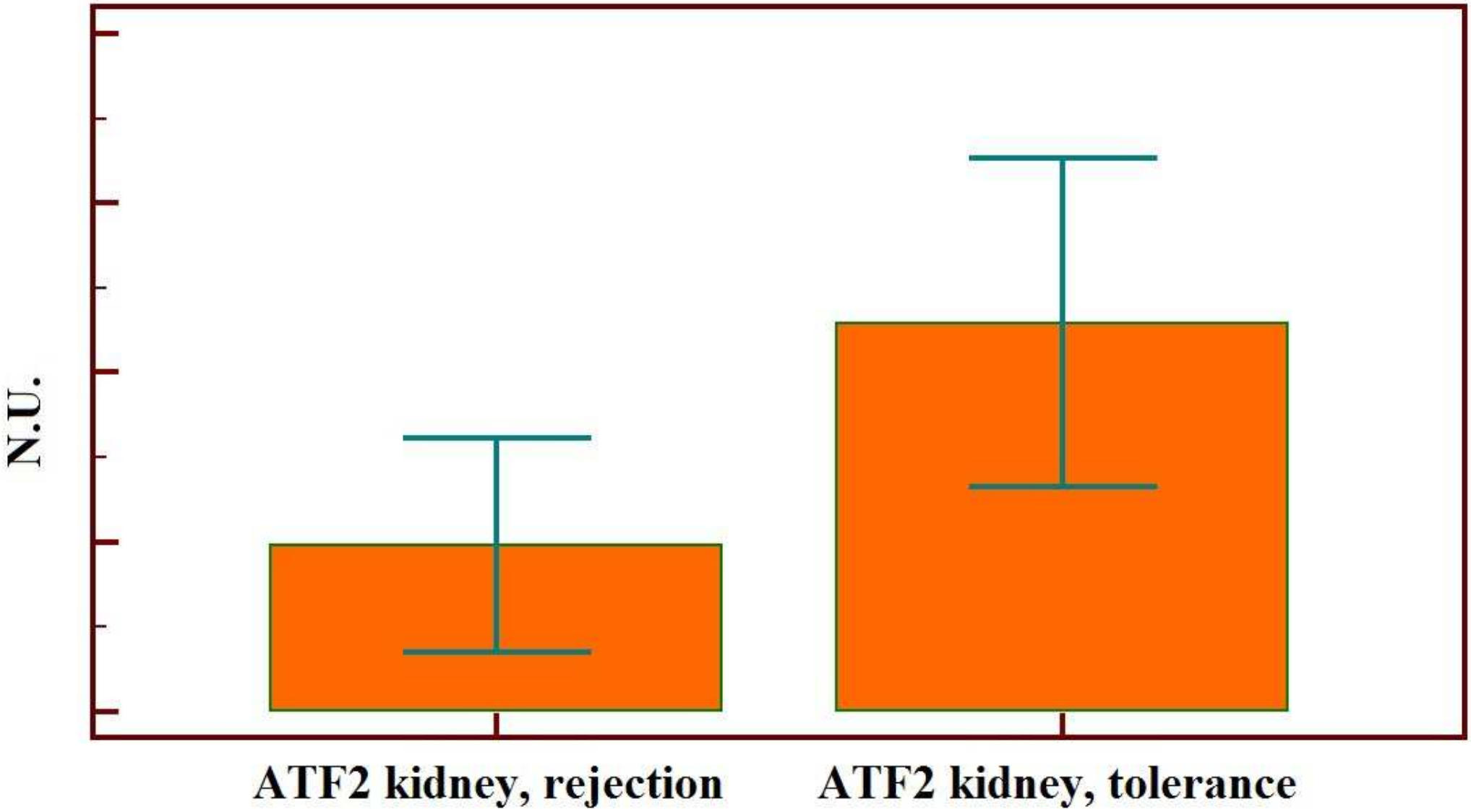


Figure 5. ATF2 profile expression, which is differentially expressed between tolerant patients and those who have rejected renal graft. It is a predictor only in kidney.

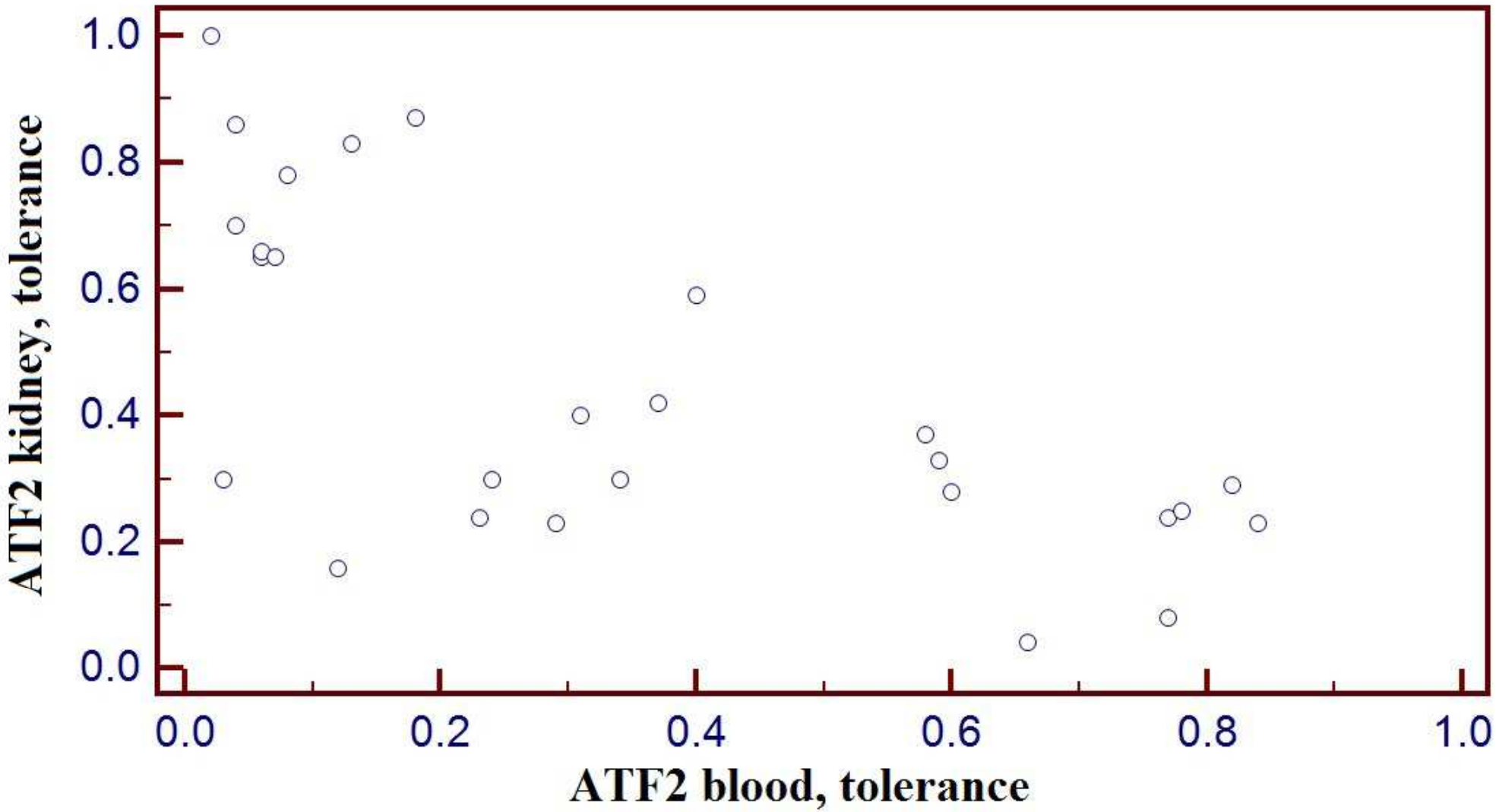
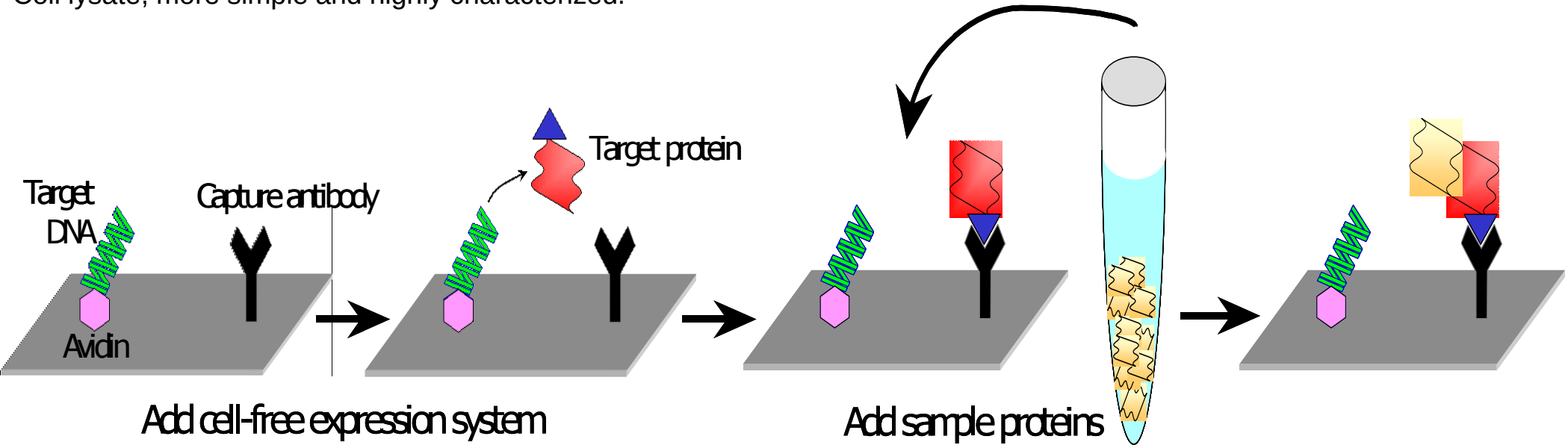


Figure 6. Scatterplot showing the Pearson's correlation between ATF2 tolerance profile expression in kidney and in peripheral blood.

Figure 3: . NAPPA technology. In each spot of NAPPA there is a plasmid DNA biotinylated that is bound to the complex BSA-streptavidin that covers the array surface; in each spot there are also present antiGST antibodies useful for the binding of the freshly expressed proteins that are tagged, at one of their ends, with a GST tail. The proteins are translated using a T7-coupled rabbit reticulocyte lysate *in vitro* transcription-translation (IVTT) system. Once bounded the query proteins the array is employed to study protein-protein interactions: sample proteins are added to the array and after the washing the array is analyzable trough label-free methods. Under study is the possibility to replace the transcription-translation system with a E. Coli lysate, more simple and highly characterized.



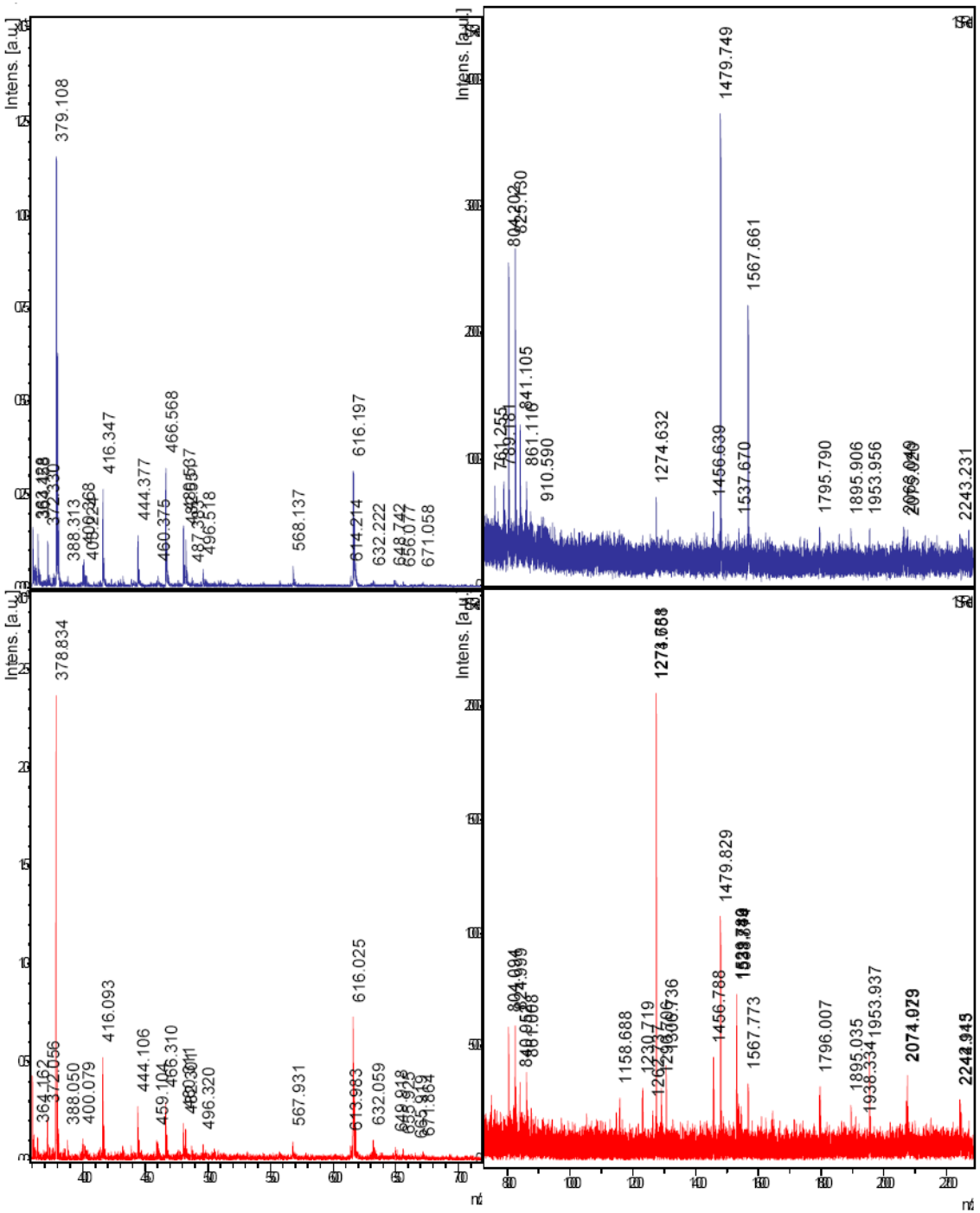


Figure 4. MALDI TOF Spectra of NAPPA after protein triptych digestion, 5–20 kDa range, for p53 (upper,left) versus A (bottom,left) samples.

Figure1 Experimental set-up. Samples were printed on a gold coated glass slides; the array printing was realized in a special geometry for MS analysis. The spots of 300 microns were printed in 12 boxes of 7 × 7 or 10x10 (spaced of 350 microns, centre to centre). The spots in a box were of the same gene: four boxes were printed with sample genes (p53, CDK2, Src-SH2 and PTPN11-SH2), two boxes were printed with master mix (MM) as negative control and reference samples, and six boxes, labelled with the letters from A to F, were printed with the sample genes in an order blinded to the researcher. SNAP-NAPPAs were analyzed by LC-ESI and MALDI-TOF MS. We utilized two MALDI-TOF MSs, a Voyager and a Bruker MS. For LC-ESI MS and Voyager MS analysis the sample were collected at the end of trypsin digestion and stored liquid in Eppendorf tubes since the analysis. For Bruker MS analysis the matrix was mixed with the trypsin digested fragment solutions directly on the slides and let to dry before the analysis.

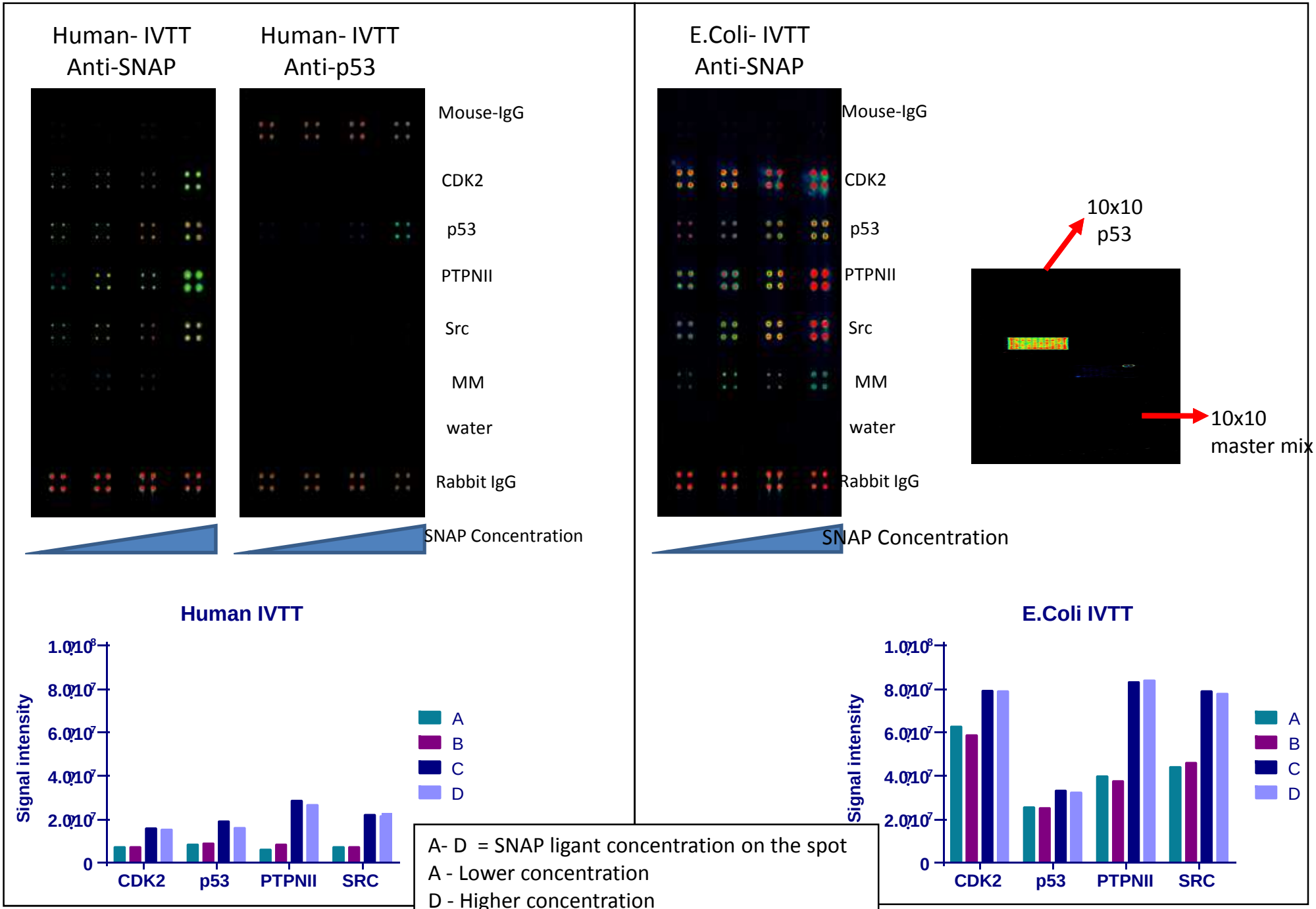
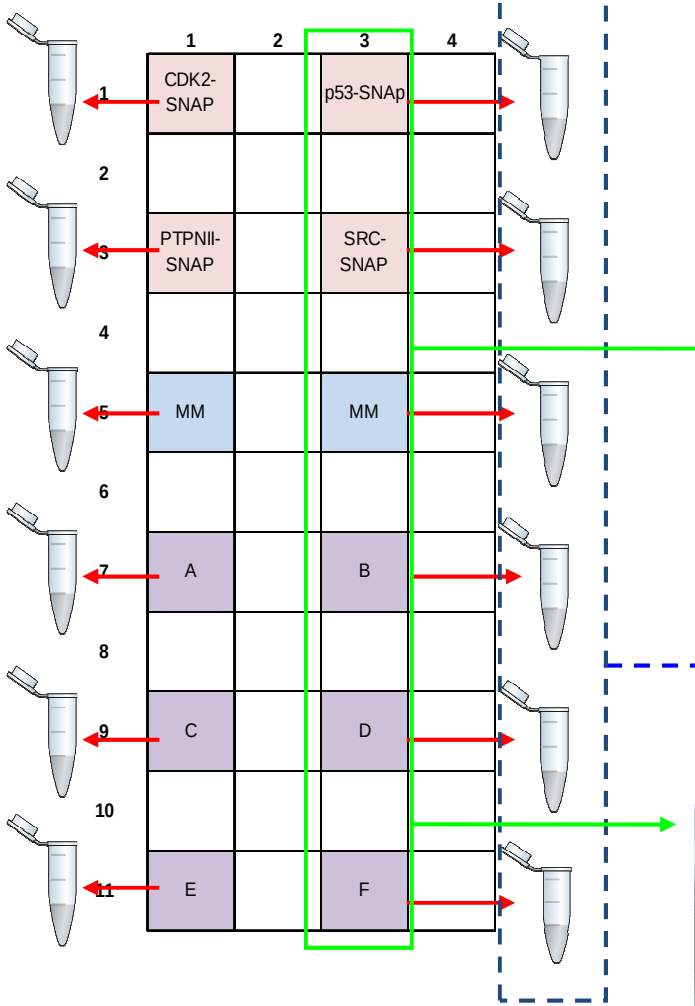


Figure 2 Fluorescence analysis of SNAP-NAPPA a) Proteins were synthesized by two different IVTT systems, 1-Step Human Coupled IVT (HCIVT) and *E. coli* IVTT. Slide images were obtain with PowerScanner and the signal intensity was quantified using the Array-ProAnalyzer 6.3. The median intensity across the quadruplicates was measured and the background was corrected throu the subtraction of the median value of the negative control with a matching SNAP concentration. b) Proteins yield for different SNAP concentrations, for HCIVT and *E. coli* IVTT systems. c) The master mix box (spotted with all the reagents of the regular NAPPA spotting mix, except DNA) was the negative control and reference box.



MALDI-TOF
Voyager

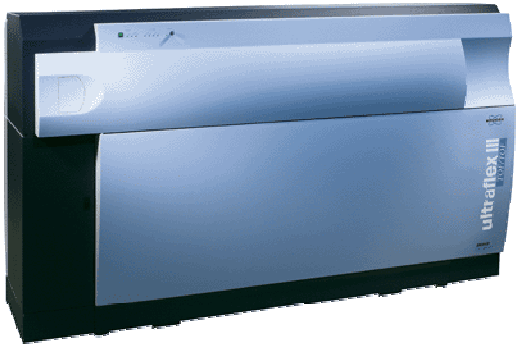




MALDI-TOF
Autoflex Bruker

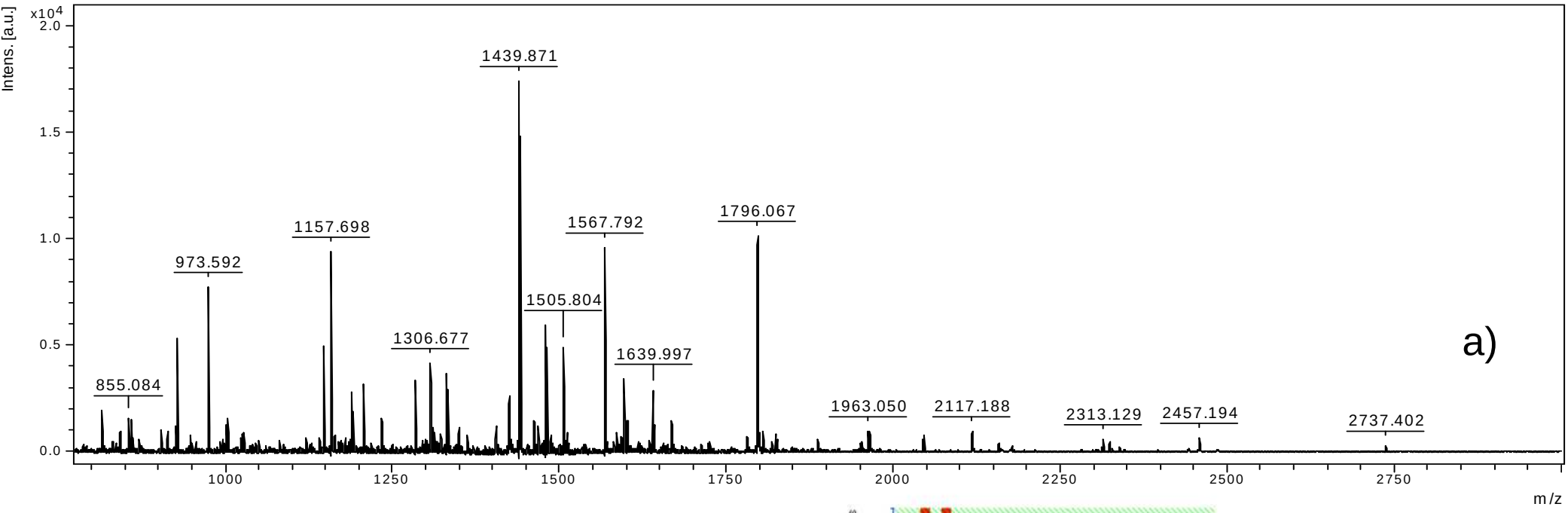
Lc-ESI MS/MS

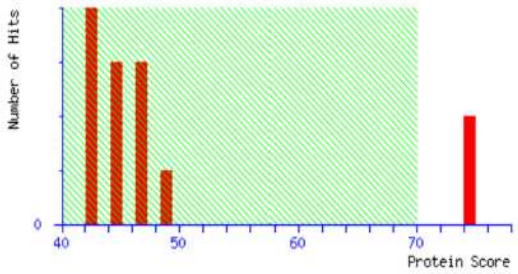




MALDI-TOF
ULTRAFLEXIII Bruker

Figure 3 : a) P53 sample spectrum obtained by Voyager MS. MASCOT data-bank results: (b) elongation factor EFTU and (c) albumin bovin present respectivly in the lysate and on the array surface. The results obtained identify p53 with a percentage of sequence coverage of 6% while for -SRC-SH2 and PTPN11- SH2 samples no fragments were identified.





Concise Protein Summary Report

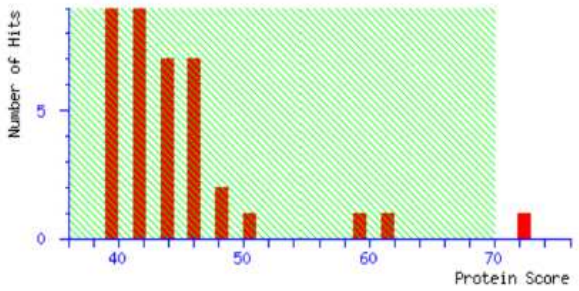
Format As | Concise Protein Summary | Help

Significance threshold p< 0.05 Max. number of hits AUTO

Re-Search All | Search Unmatched

1. EFTU_CROS8 **Mass:** 43177 **Score:** 74 **Expect:** 0.019 **Matches:** 7
Elongation factor Tu OS=Cronobacter sakazakii (strain ATCC BAA-894) GN=tuf1 PE=3 SV=1

b)



Concise Protein Summary Report

Format As | Concise Protein Summary | Help

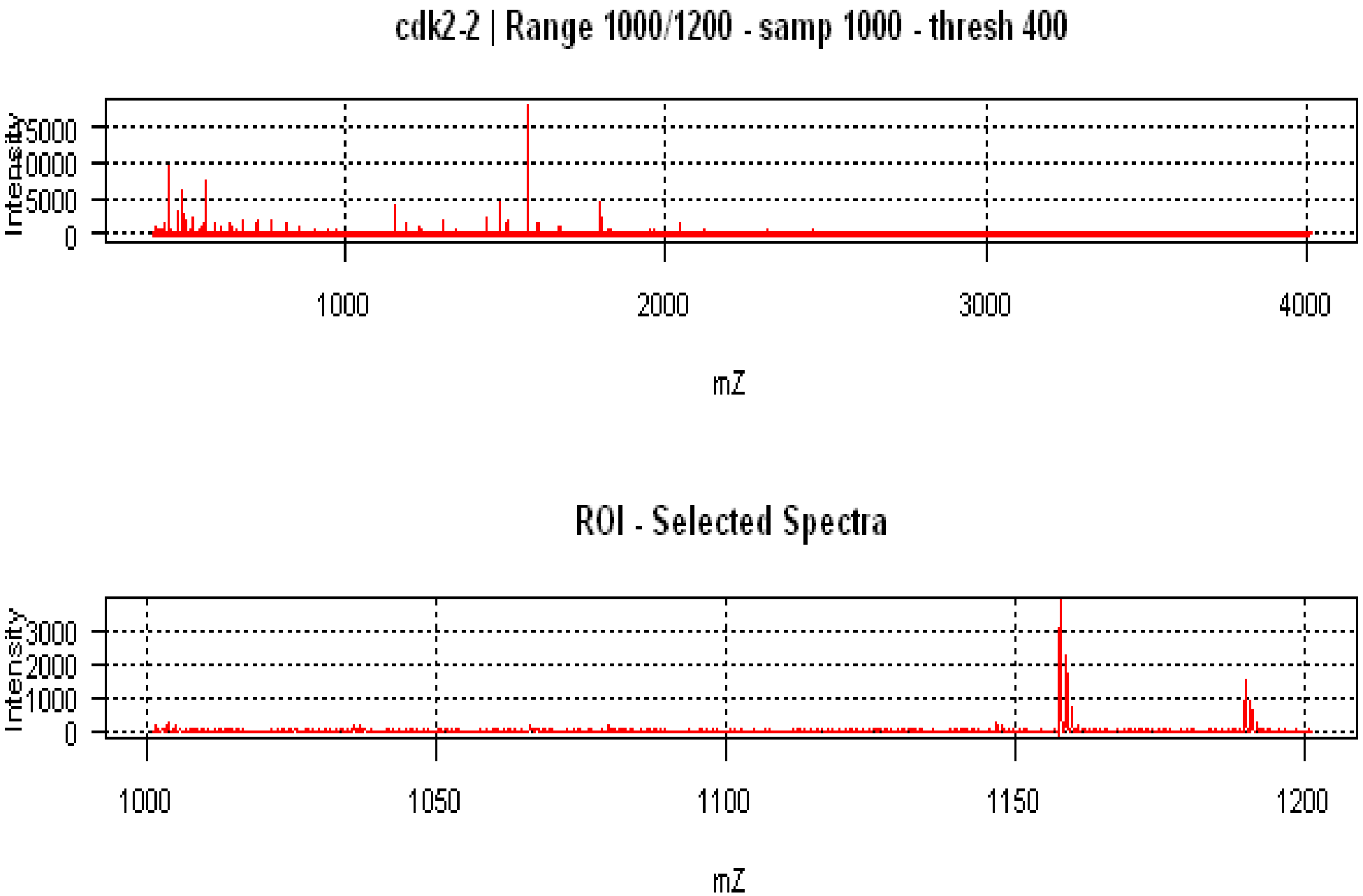
Significance threshold p< 0.05 Max. number of hits AUTO

Re-Search All | Search Unmatched

1. ALBU_BOVIN **Mass:** 69248 **Score:** 72 **Expect:** 0.032 **Matches:** 13
Serum albumin OS=Bos taurus GN=ALB PE=1 SV=4

c)

Figure 4 Experimental mass list of CDK2 (ultraflex data) and experimental mass list [MM+ lysate] (ultraflex data) on the top. ROI selection 1000/1200 of spectra. The results obtained allow us to identify CDK2 sample with a percentage of sequence coverage of 22% .



Protein score is -10*Log(P), where P is the probability that the observed match is a random event.
Protein scores greater than 70 are significant (p<0.05).

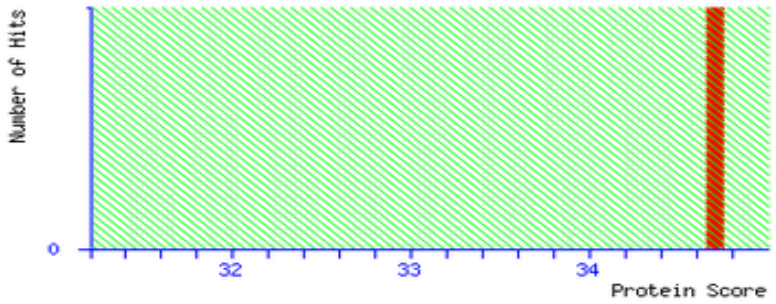


Figure 5 CDK2 sample spectrum obtained by Voyager MS. MASCOT data-bank results: highlighted by red arrow is the homologous kinase (CSK2) proteins found.

1. TRI74_HUMAN Mass: 28528 Score: 35 Expect: 1.8e+02 Matches: 2
Tripartite motif-containing protein 74 OS=Homo sapiens GN=TRIM74 PE=2 SV=1
NUBP2_DICDI Mass: 28944 Score: 34 Expect: 2e+02 Matches: 2
Cytosolic Fe-S cluster assembly factor NUBP2 homolog OS=Dictyostelium discoideum GN=nubp2 PE=3 SV=1
TRI73_HUMAN Mass: 28498 Score: 34 Expect: 2e+02 Matches: 2
Tripartite motif-containing protein 73 OS=Homo sapiens GN=TRIM73 PE=2 SV=1
SPRTL_STRT1 Mass: 17445 Score: 33 Expect: 2.8e+02 Matches: 2
Protein SprT-like OS=Streptococcus thermophilus (strain CNRZ 1066) GN=str0664 PE=3 SV=1
SPRTL_STRT2 Mass: 17445 Score: 33 Expect: 2.8e+02 Matches: 2
Protein SprT-like OS=Streptococcus thermophilus (strain ATCC BAA-250 / LMG 18311) GN=stu0664 PE=3 SV=1
SPRTL_STRTD Mass: 17445 Score: 33 Expect: 2.8e+02 Matches: 2
Protein SprT-like OS=Streptococcus thermophilus (strain ATCC BAA-491 / LMD-9) GN=STER_0717 PE=3 SV=1
PCNA_THEAC Mass: 27564 Score: 33 Expect: 2.8e+02 Matches: 2
DNA polymerase sliding clamp OS=Thermoplasma acidophilum (strain ATCC 25905 / DSM 1728 / JCM 9062 / NBRC 15155 / AMRC-C165) GN=pcn PE=3 SV=1
Y1241_PHOPR Mass: 29086 Score: 32 Expect: 3.1e+02 Matches: 2
UPF0176 protein PBPRA1241 OS=Photobacterium profundum GN=PBPRA1241 PE=3 SV=1
PDGFC_MOUSE Mass: 38717 Score: 32 Expect: 3.5e+02 Matches: 2
Platelet-derived growth factor C OS=Mus musculus GN=Pdgfc PE=1 SV=2
WDR92_MOUSE Mass: 39765 Score: 31 Expect: 4.1e+02 Matches: 2
WD repeat-containing protein 92 OS=Mus musculus GN=Wdr92 PE=2 SV=1
Y371_DESOH Mass: 26873 Score: 31 Expect: 4.6e+02 Matches: 2
Probable transcriptional regulatory protein Dole_0371 OS=Desulfococcus oleovorans (strain DSM 6200 / Hxd3) GN=Dole_0371 PE=3 SV=1
Y3107_SHEWM Mass: 43767 Score: 30 Expect: 4.9e+02 Matches: 2
Putative reductase Swoo_3107 OS=Shewanella woodyi (strain ATCC 51908 / MS32) GN=Swoo_3107 PE=3 SV=1
Y3256_SHEPW Mass: 43887 Score: 30 Expect: 4.9e+02 Matches: 2
Putative reductase swp_3256 OS=Shewanella piezotolerans (strain WP3 / JCM 13877) GN=swp_3256 PE=3 SV=1
HUTI_RHILO Mass: 42959 Score: 30 Expect: 5.2e+02 Matches: 2
Imidazolonepropionase OS=Rhizobium loti (strain MAFF303099) GN=hutI PE=3 SV=1
YUC9_ARATH Mass: 47371 Score: 29 Expect: 6.2e+02 Matches: 2
Probable indole-3-pyruvate monooxygenase YUCCA9 OS=Arabidopsis thaliana GN=YUC9 PE=2 SV=1
ANGL1_BOVIN Mass: 56638 Score: 29 Expect: 6.8e+02 Matches: 2
Angiopoietin-related protein 1 OS=Bos taurus GN=ANGPTL1 PE=2 SV=1
DNAJ_ACTS2 Mass: 41058 Score: 29 Expect: 7.3e+02 Matches: 2
Chaperone protein DnaJ OS=Actinobacillus succinogenes (strain ATCC 55618 / 130Z) GN=dnaJ PE=3 SV=1
TPZ1_SCHPO Mass: 57649 Score: 28 Expect: 7.8e+02 Matches: 2
Protection of telomeres protein tpz1 OS=Schizosaccharomyces pombe (strain 972 / ATCC 24843) GN=tpz1 PE=1 SV=2
RL2_SPHWW Mass: 30357 Score: 28 Expect: 8e+02 Matches: 2
50S ribosomal protein L2 OS=Sphingomonas wittichii (strain RW1 / DSM 6014 / JCM 10273) GN=rplB PE=3 SV=1
CSK2A_SPOFR Mass: 41998 Score: 28 Expect: 8.2e+02 Matches: 2
Casein kinase II subunit alpha OS=Spodoptera frugiperda PE=2 SV=1
DDL_HELP2 Mass: 39679 Score: 28 Expect: 8.6e+02 Matches: 2
D-alanine--D-alanine ligase OS=Helicobacter pylori (strain P12) GN=ddl PE=3 SV=1
YUC5_ARATH Mass: 47411 Score: 28 Expect: 8.6e+02 Matches: 2
Probable indole-3-pyruvate monooxygenase YUCCA5 OS=Arabidopsis thaliana GN=YUC5 PE=2 SV=1

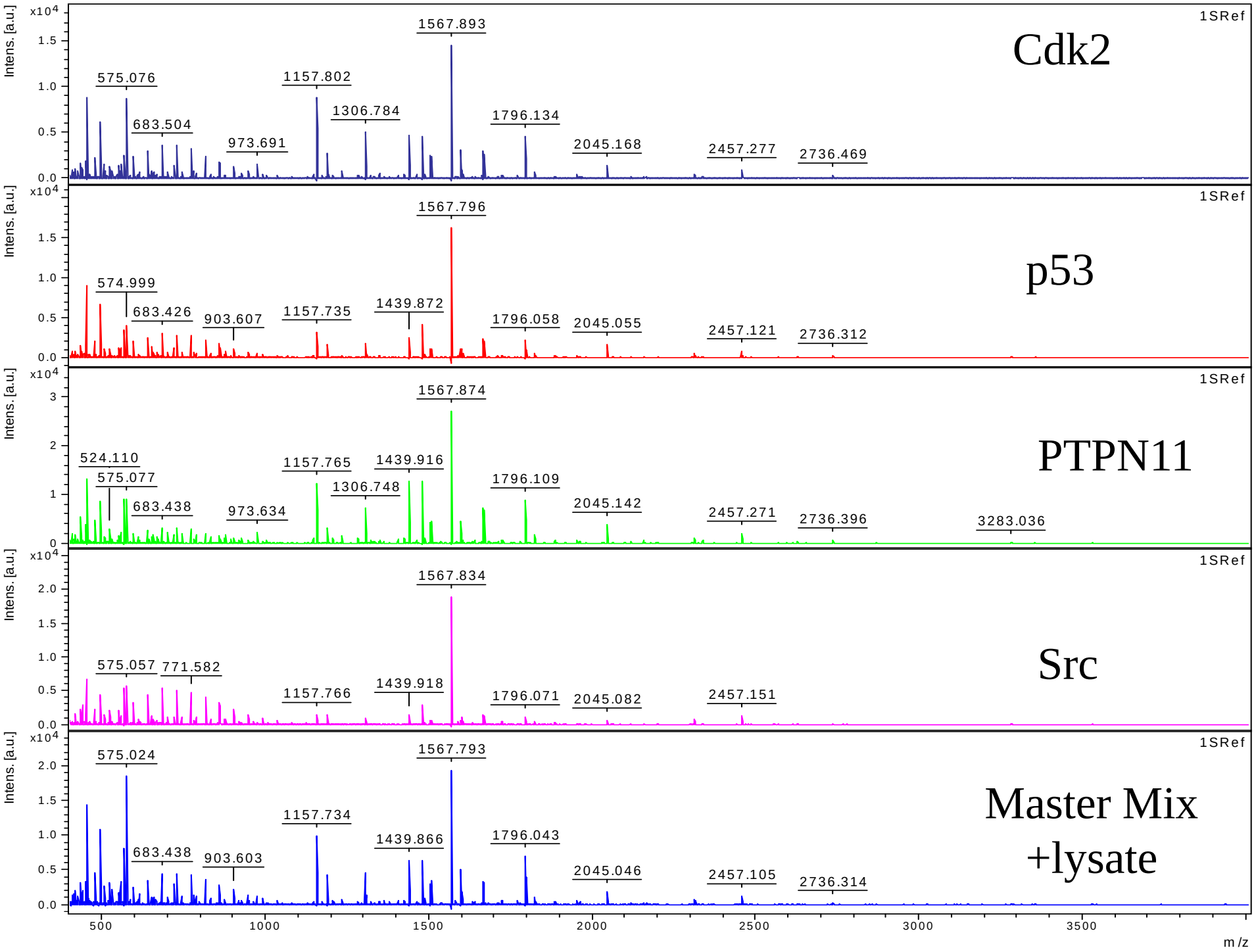


Fig. 6a Samples mass spectra acquired by Ultraflex III MS. Each one of this spectrum is the sum of 100 single shot spectrum a) full range; b) 1.1 - 2.4 kDa range

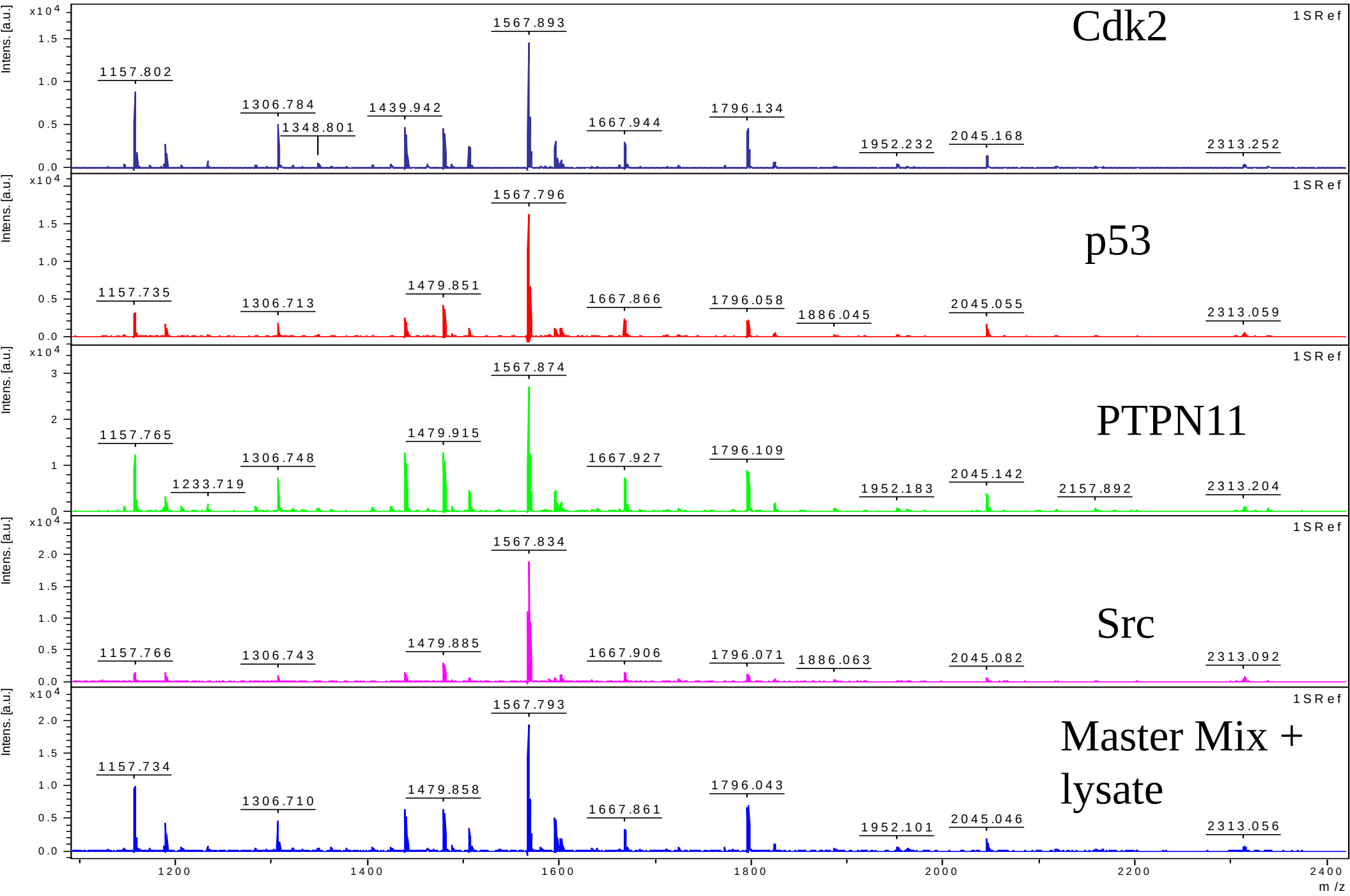


Fig. 6b Samples mass spectra acquired by Ultraflex III MS. Each one of this spectrum is the sum of 100 single shot spectrum a) full range; b) 1.1 - 2.4 kDa range

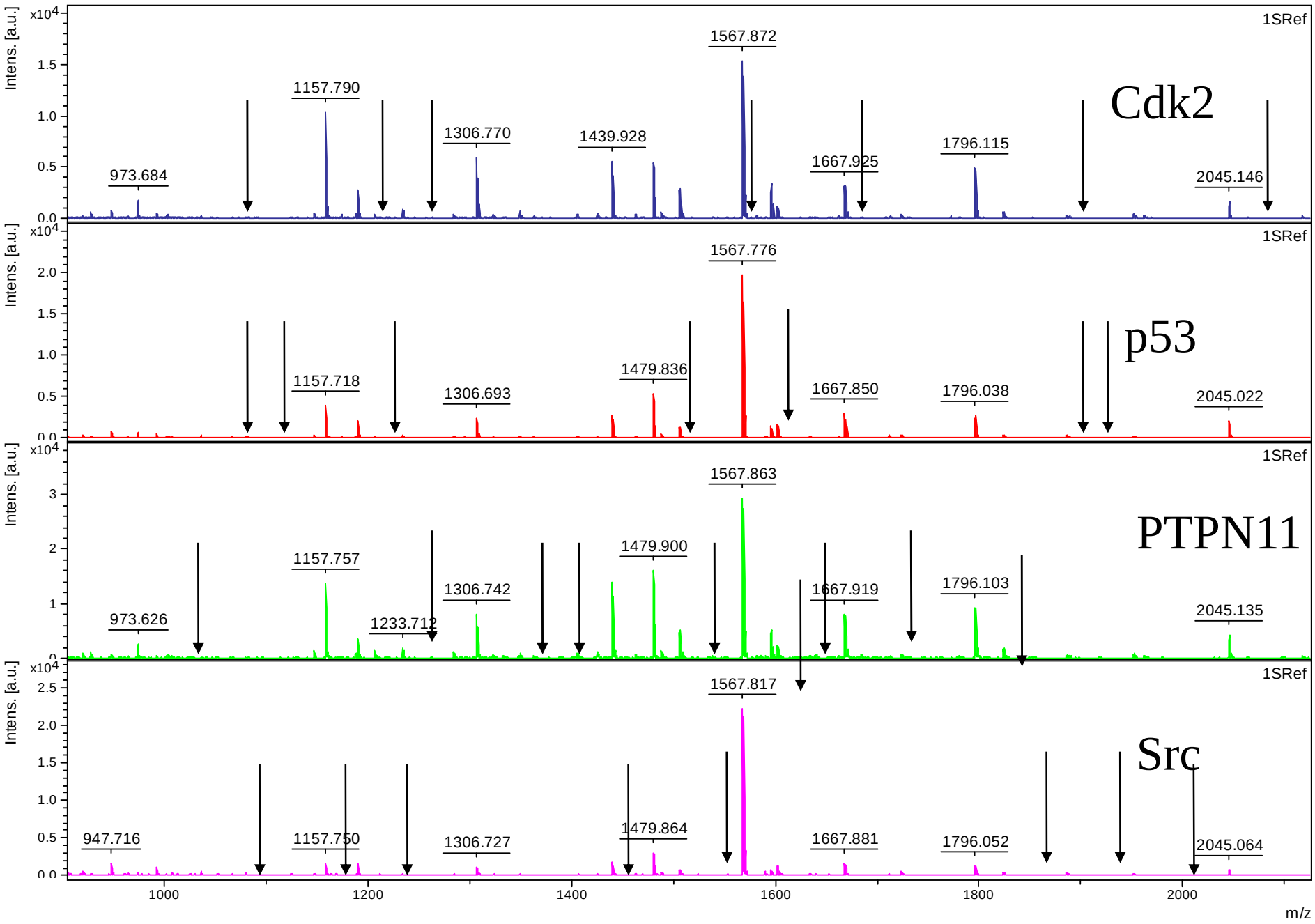


Figure 7: UltraflexIII samples mass spectra summation. The arrows point at the theoretical peak position.

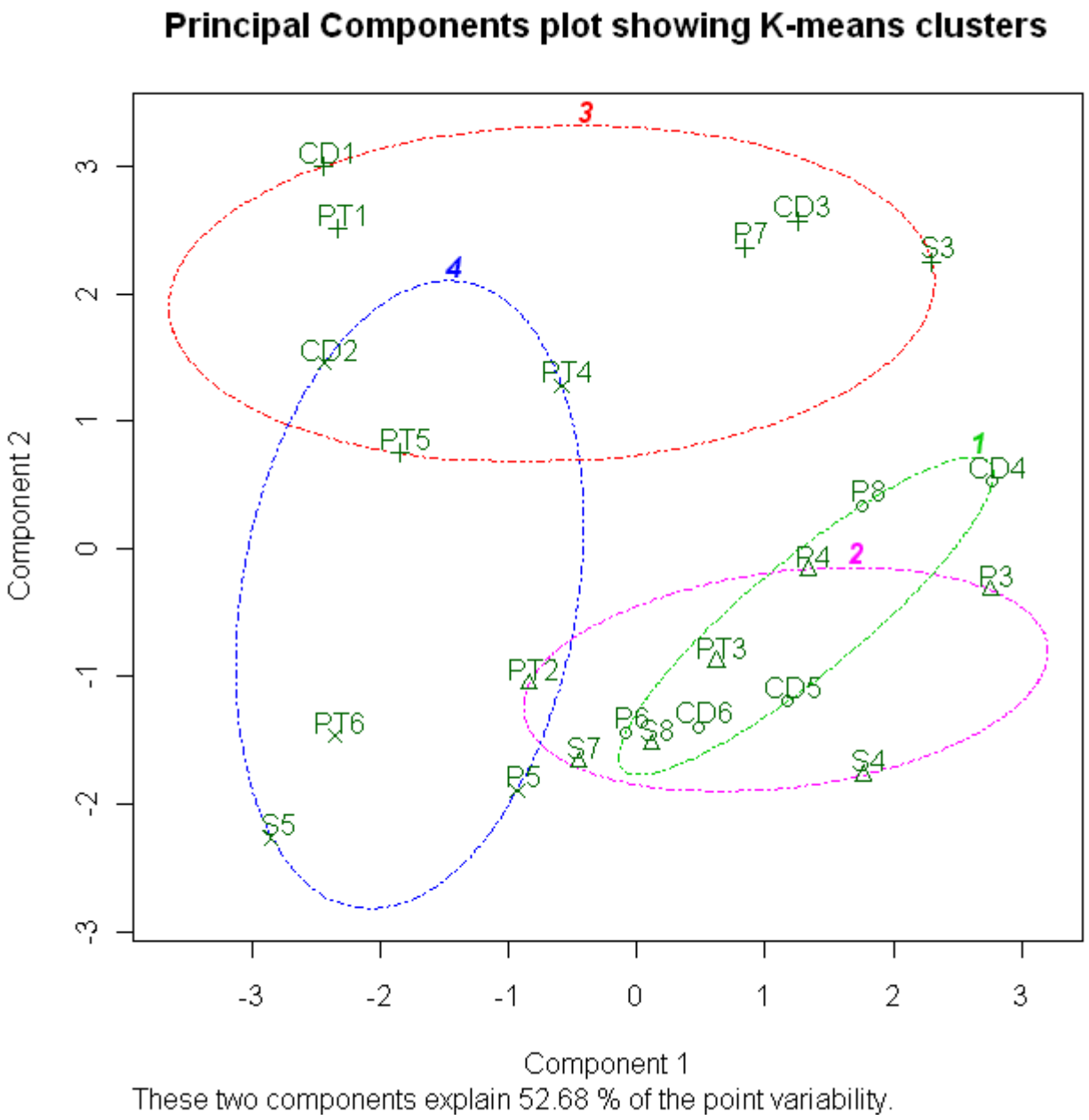


Figure 8: *SpADS and Clustering solution for a specimen of 23 protein samples of raw data. Only binning preprocessing function was performed before cluster analysis run on the ROI 1000/2000*

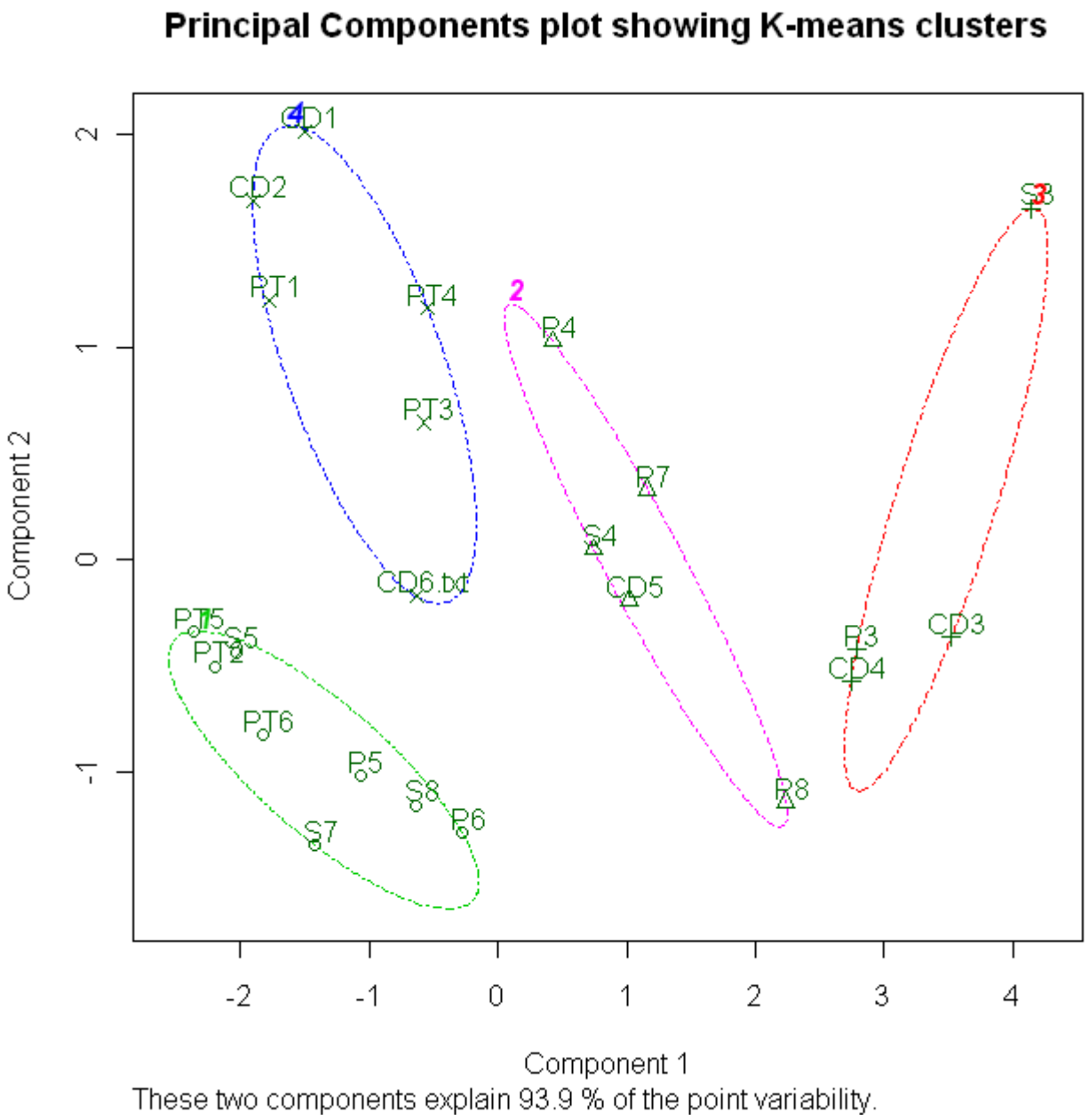


Figure 9: *SpADS and Clustering solution for a specimen of 23 protein samples of raw data. Only binning preprocessing function was performed before cluster analysis run on the ROI 1000/1200*

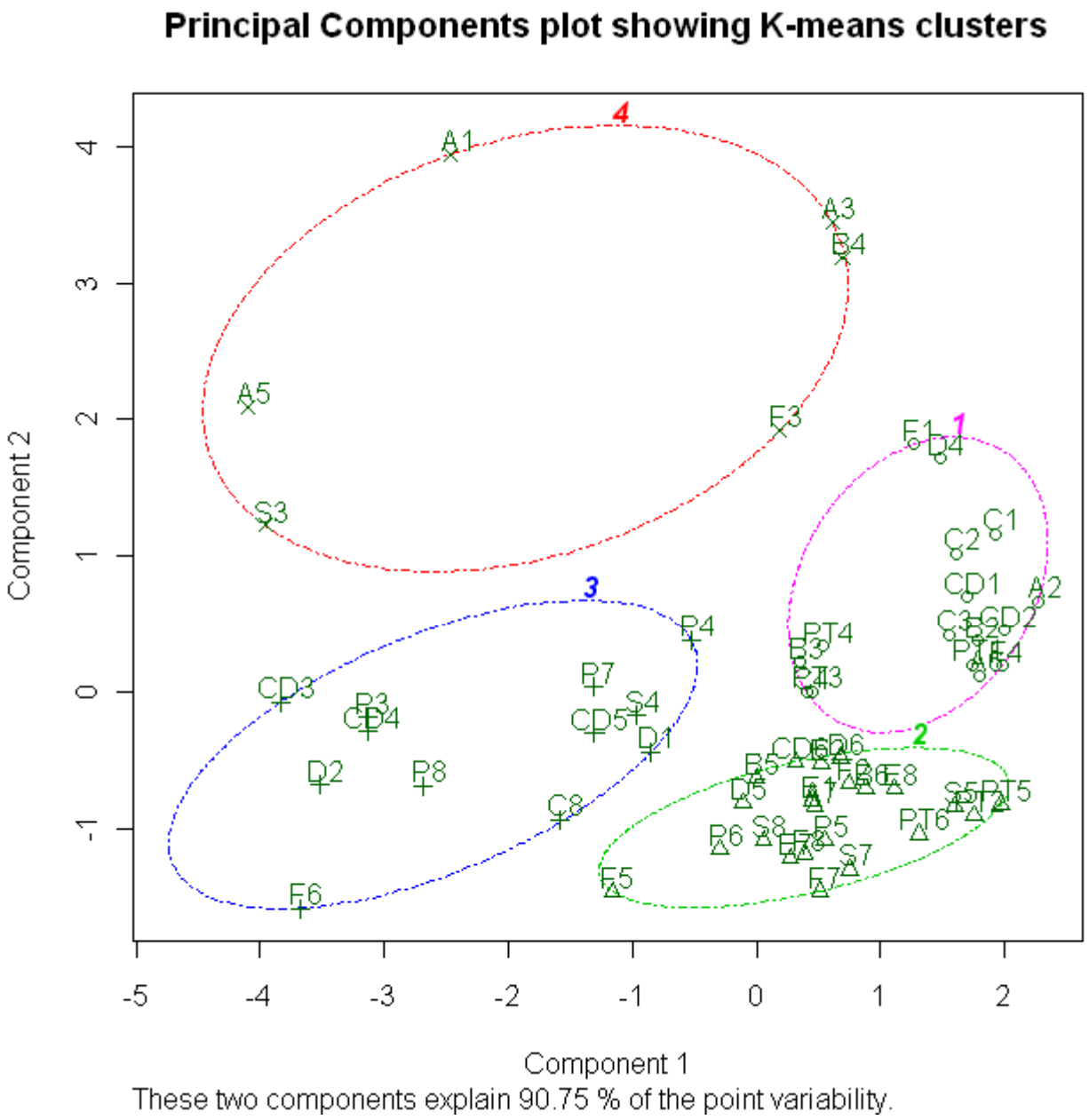


Figure 10: *SpADS and Clustering solution for a specimen of 56 protein samples of raw data. Only binning preprocessing function was performed before cluster analysis run on the ROI 1000/1200*

Figure 5. (left) Flow-cell and static dual QMC_D
(right) prototype built in house to follow each step of the protein expression versus time;



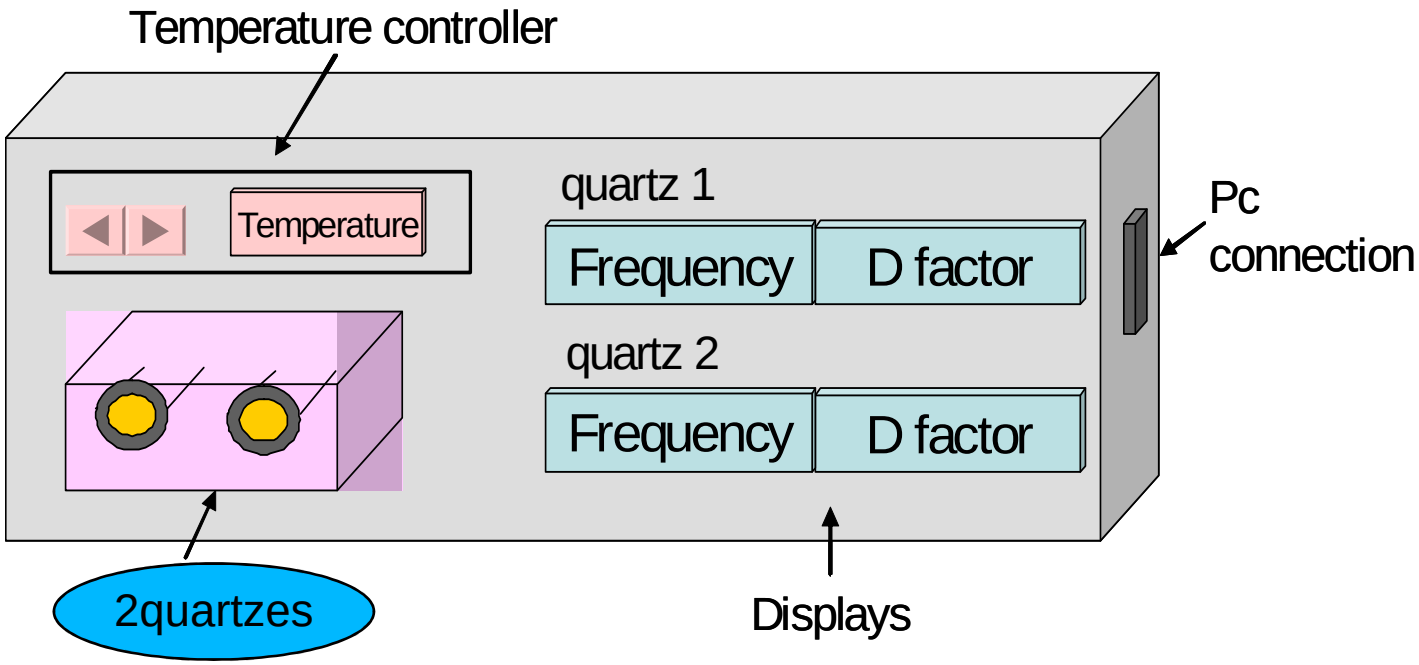
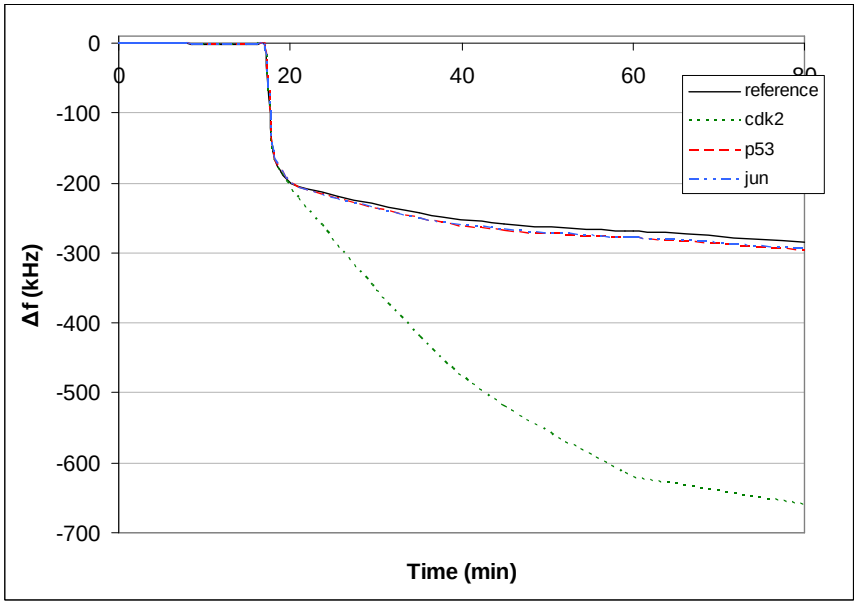
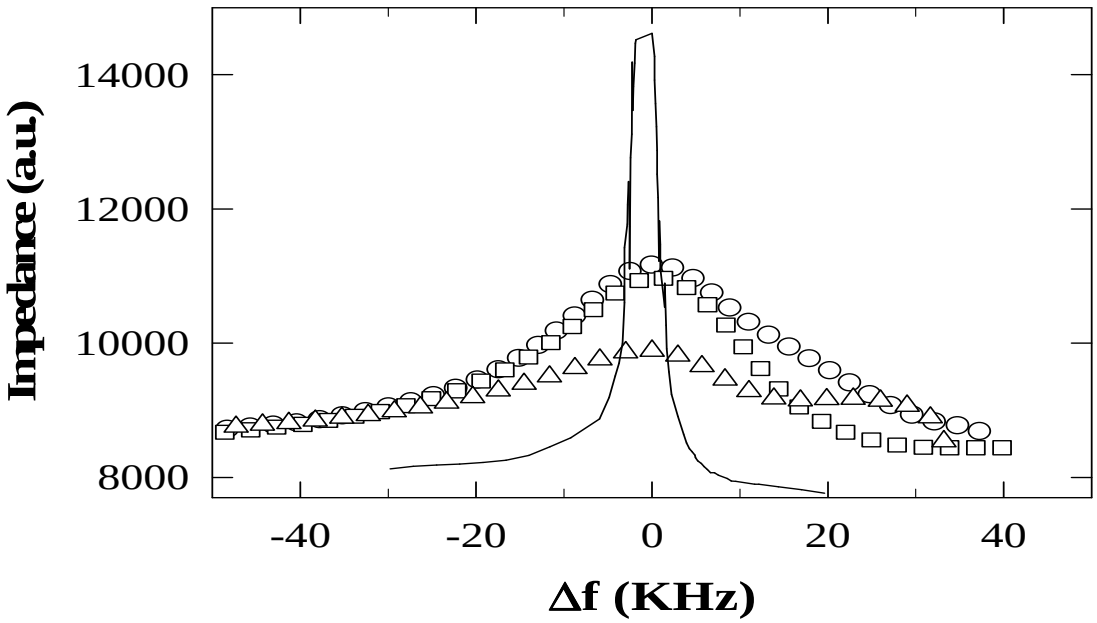
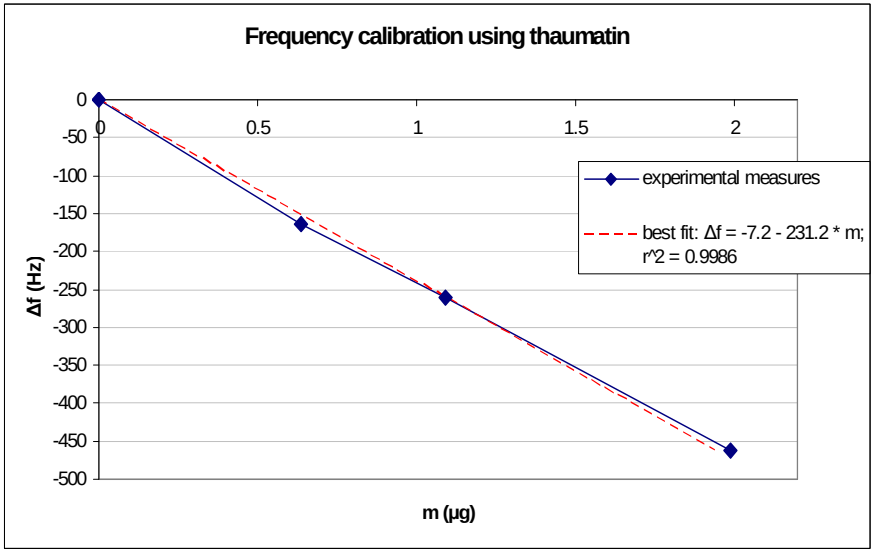
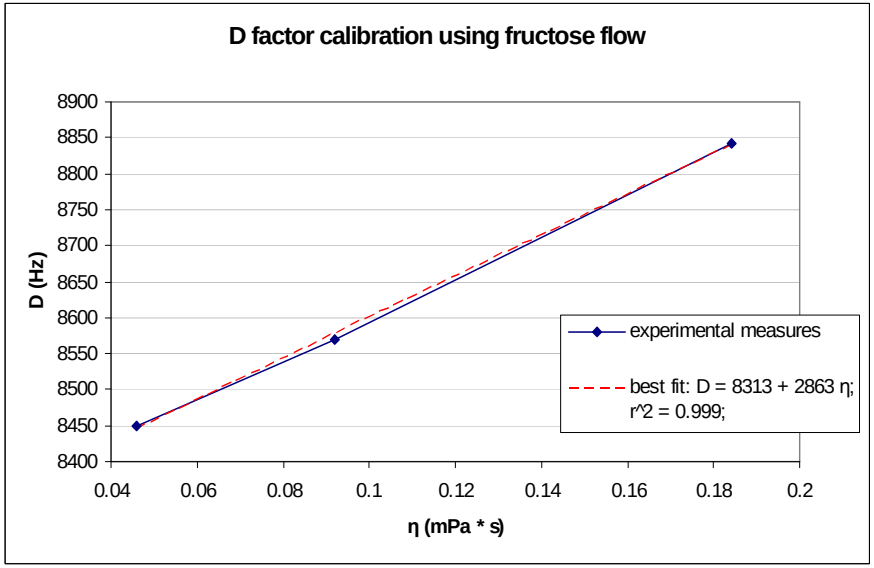


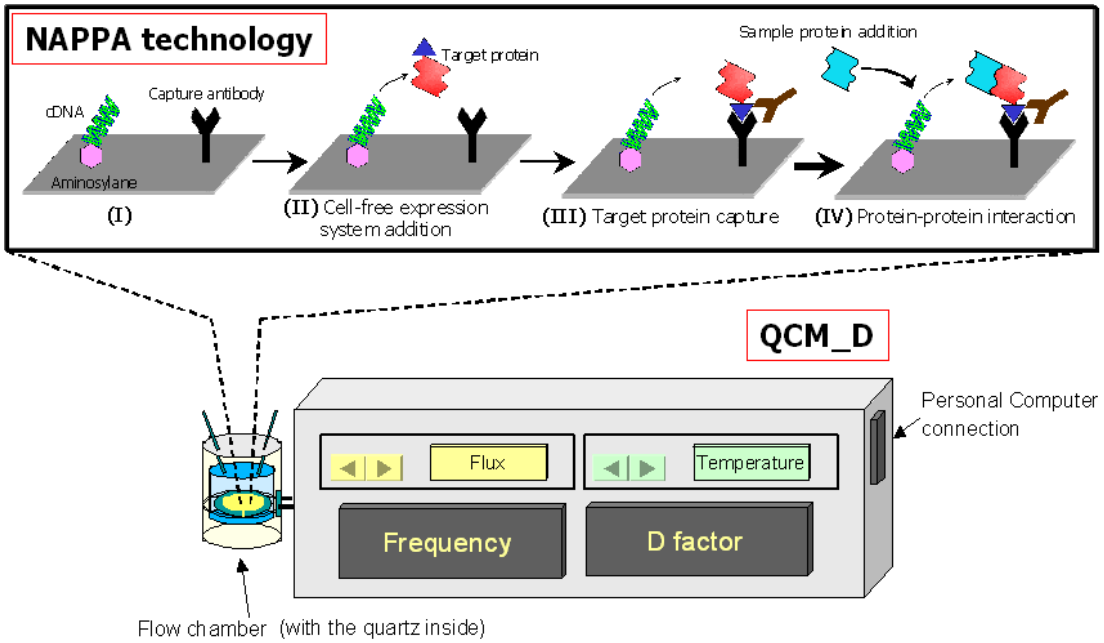
Figure 6.. (Above) Acquisition of mass via frequency versus time (left) and of quality *D* factor determined by HWHH of the impedence versus
frequency at the resonance frequency (right) for Jun, p53 and CdK2; (Below) Calibration of QMC-F and QMC-D.

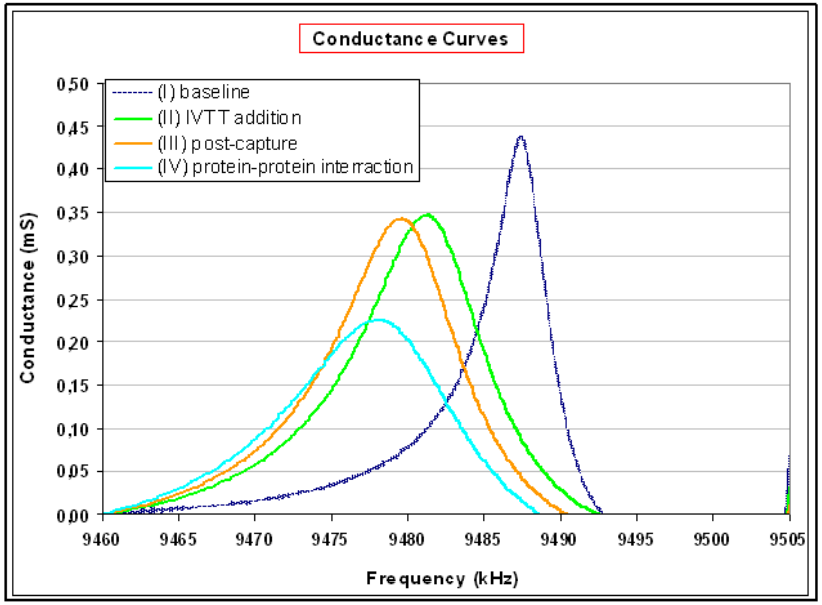









NAPPA technology
cDNA
Capture antibody
Aminosylane
(I)
Target protein
(II) Cell-free expression system addition
Sample protein addition
(III) Target protein capture
(IV) Protein-protein interaction
QCM_D
Flux
Temperature
Frequency
D factor
Personal Computer connection
Flow chamber (with the quartz inside)


Conductance Curves
(I) baseline
(II) IVTT addition
(III) post-capture
(IV) protein-protein interaction
Conductance (mS)
0.50
0.45
0.40
0.35
0.30
0.25
0.20
0.15
0.10
0.05
0.00
9460
9465
9470
9475
9480
9485
9490
9495
9500
9505
Frequency (kHz)

ABSTRACT

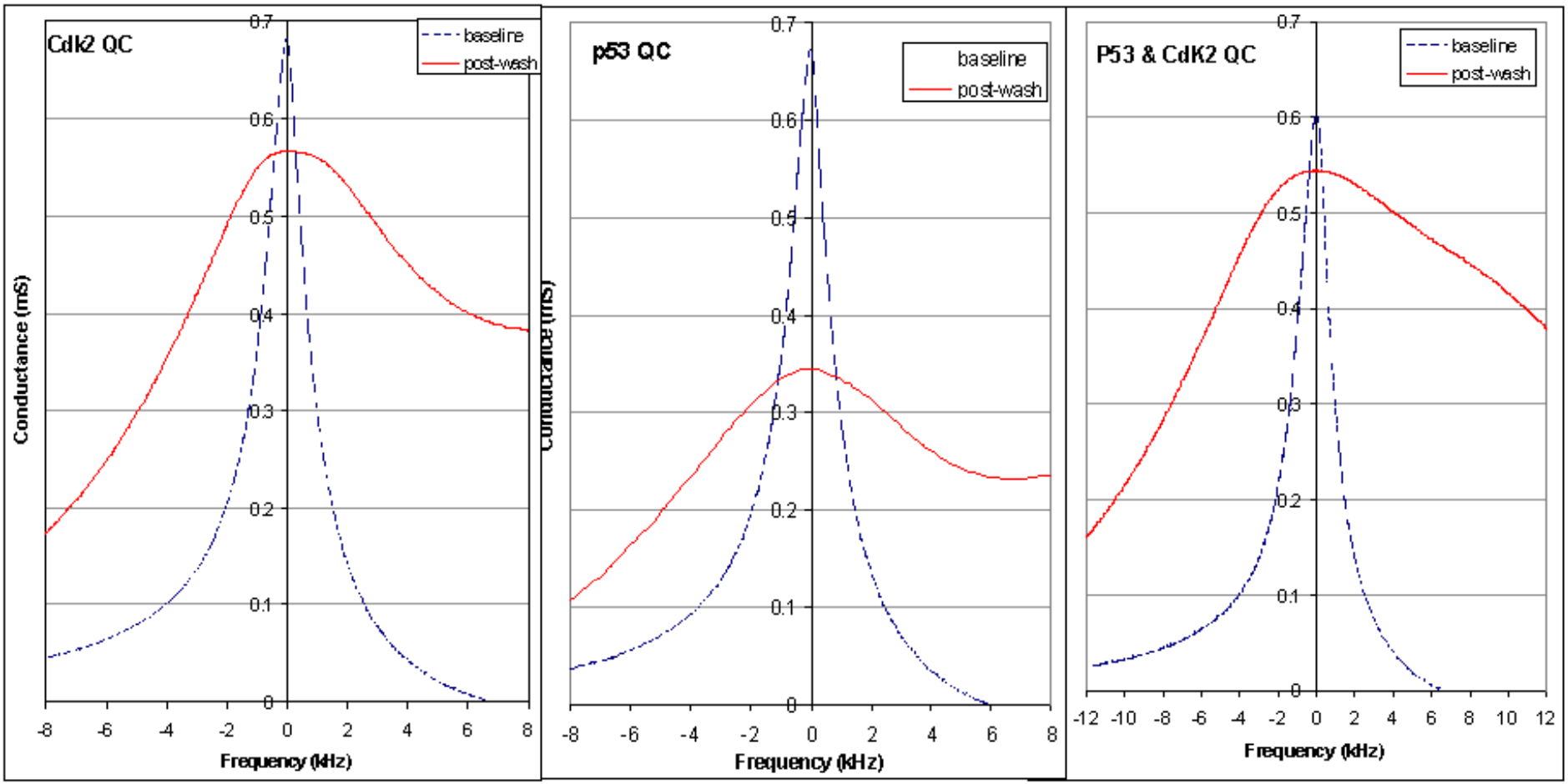

CdK2 QC
baseline
post-wash
Conductance (mS)
Frequency (kHz)
p53 QC
baseline
post-wash
Frequency (kHz)
P53 & CdK2 QC
baseline
post-wash
Frequency (kHz)

Figure 2:.

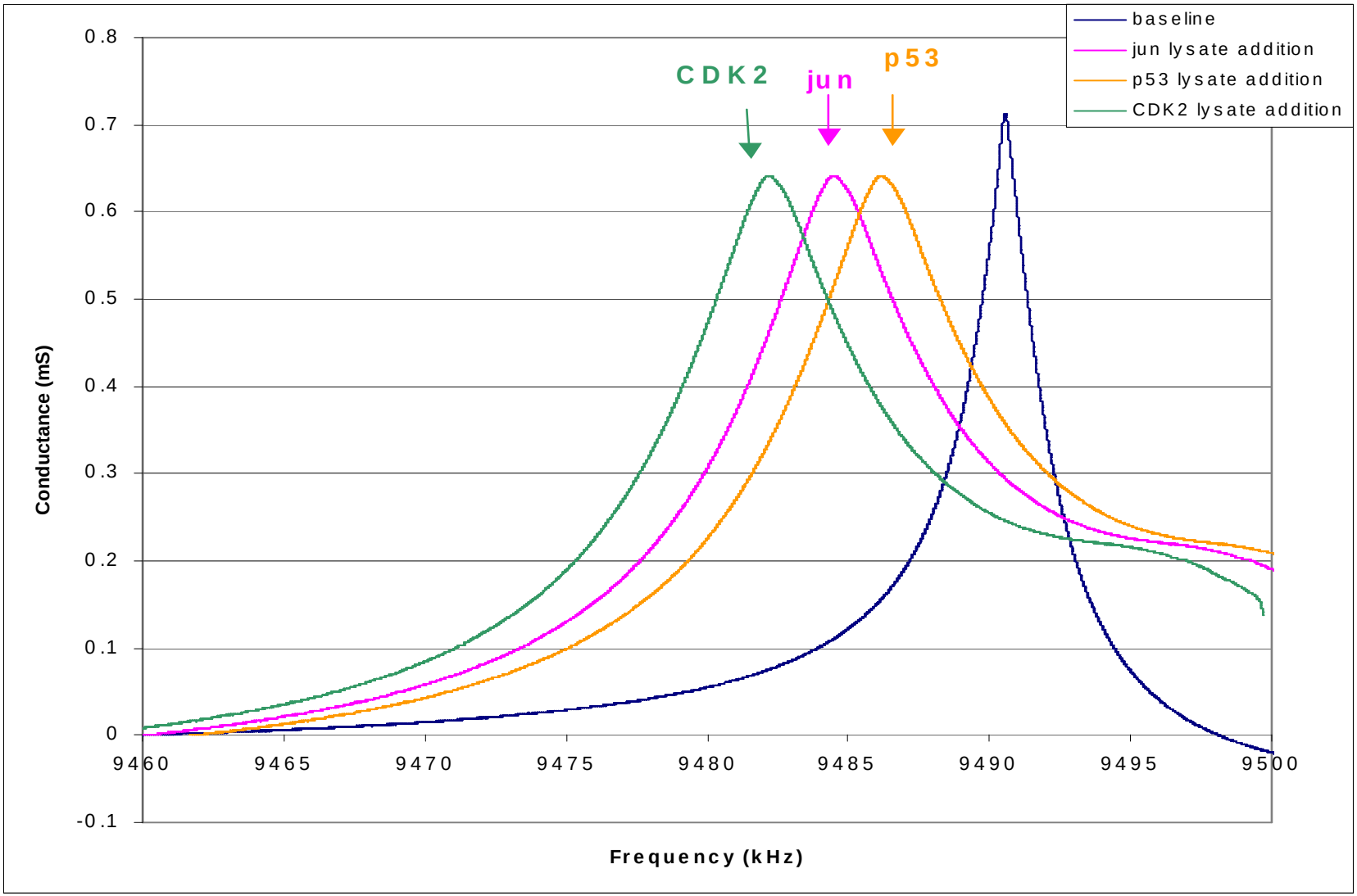

baseline
jun lysate addition
p53 lysate addition
CDK2 lysate addition
CDK2
jun
p53
0.8
0.7
0.6
0.5
0.4
0.3
0.2
0.1
0
-0.1
Conductance (mS)
9460
9465
9470
9475
9480
9485
9490
9495
9500
Frequency (kHz)

Figure 3:

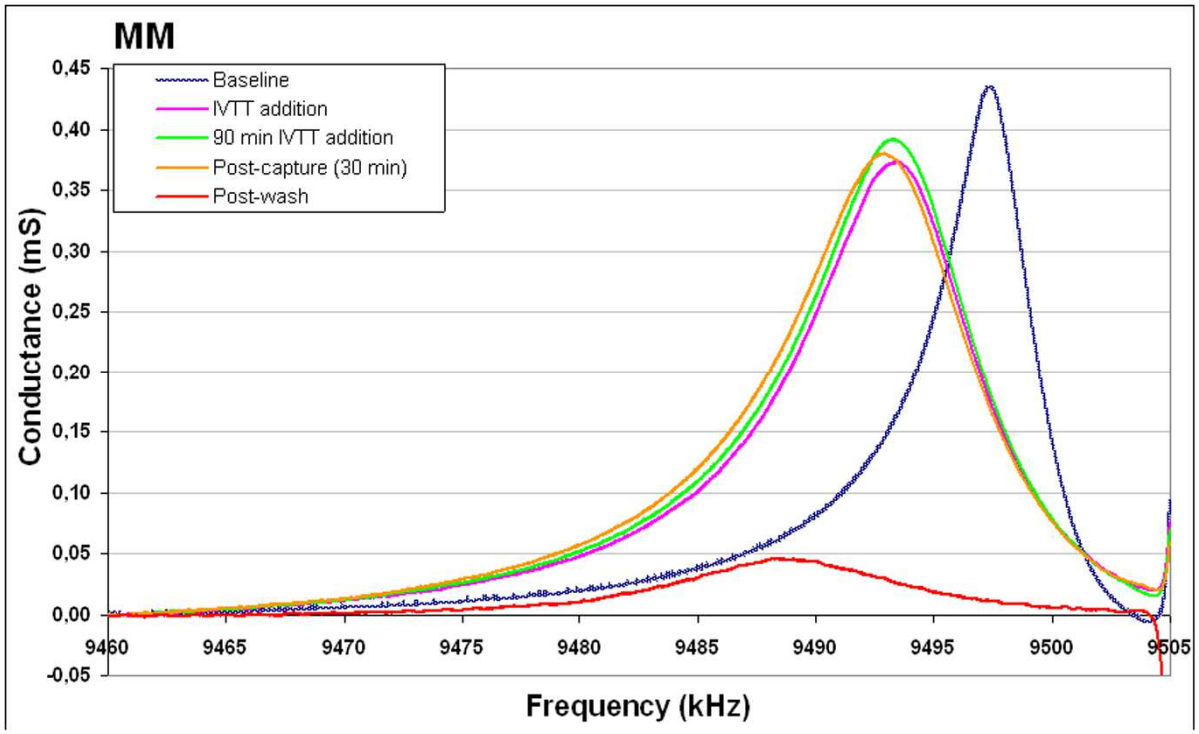
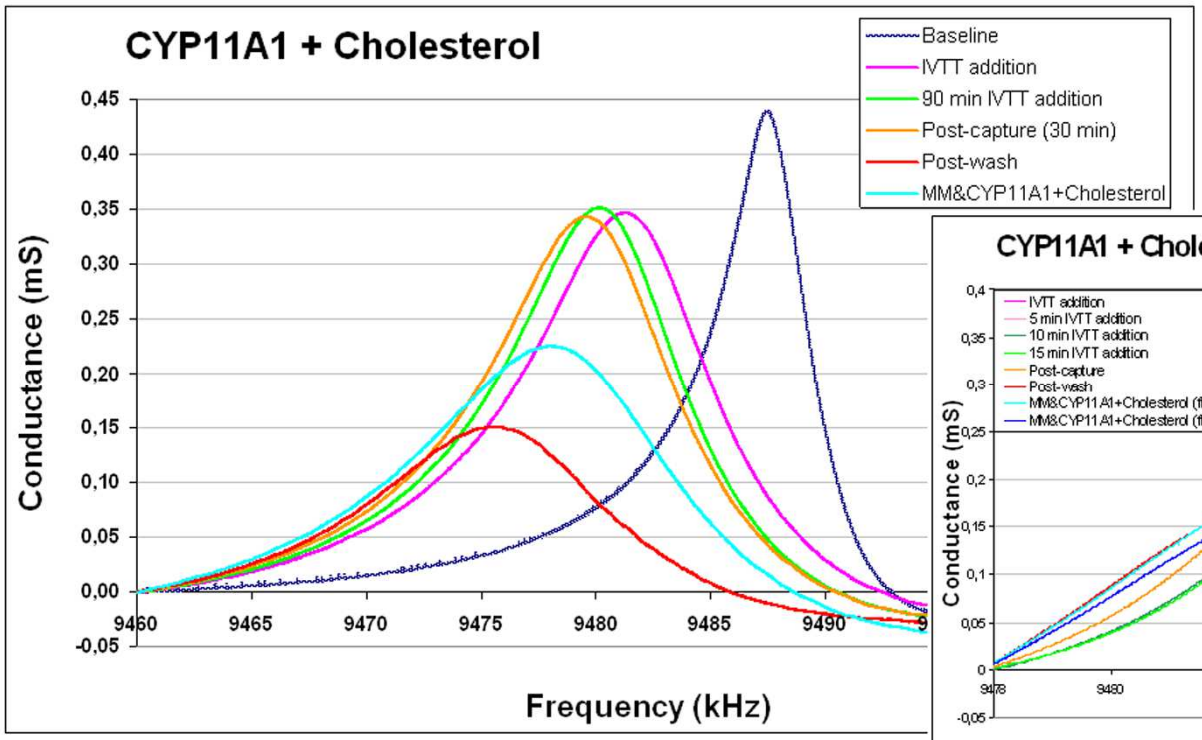
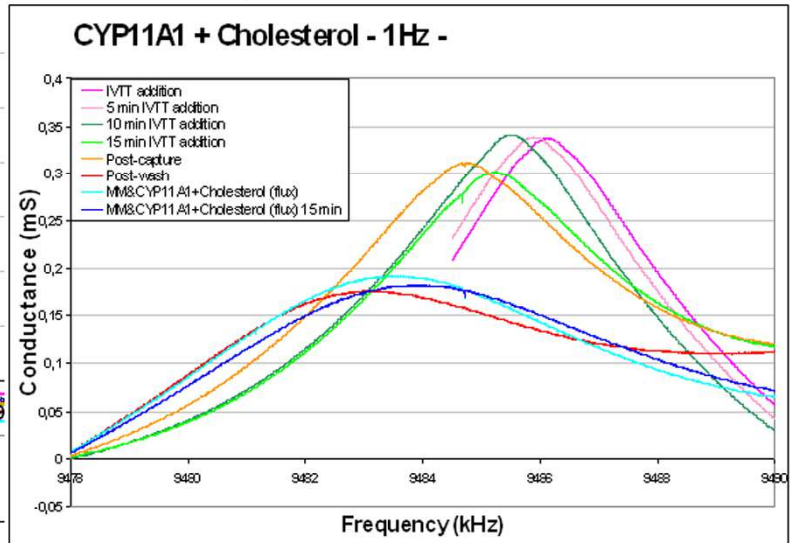
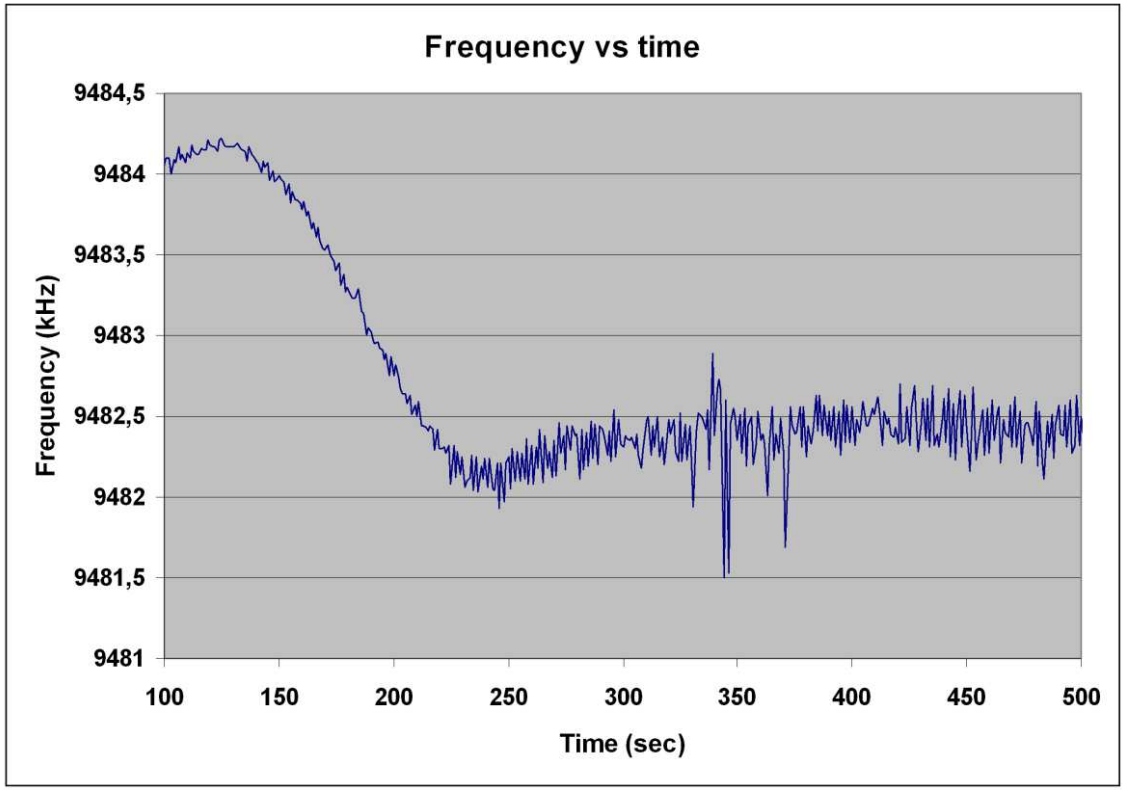

MM
Baseline
IVTT addition
90 min IVTT addition
Post-capture (30 min)
Post-wash
Conductance (mS)
Frequency (kHz)

Figure 4


CYP11A1 + Cholesterol
Baseline
IVTT addition
90 min IVTT addition
Post-capture (30 min)
Post-wash
MM&CYP11A1+Cholesterol
Conductance (mS)
Frequency (kHz)


CYP11A1 + Cholesterol - 1Hz -
IVTT addition
5 min IVTT addition
10 min IVTT addition
15 min IVTT addition
Post-capture
Post-wash
MM&CYP11A1+Cholesterol (flux)
MM&CYP11A1+Cholesterol (flux) 15 min
Conductance (mS)
Frequency (kHz)


Frequency vs time
Frequency (kHz)
9484,5
9484
9483,5
9483
9482,5
9482
9481,5
9481
100
150
200
250
300
350
400
450
500
Time (sec)

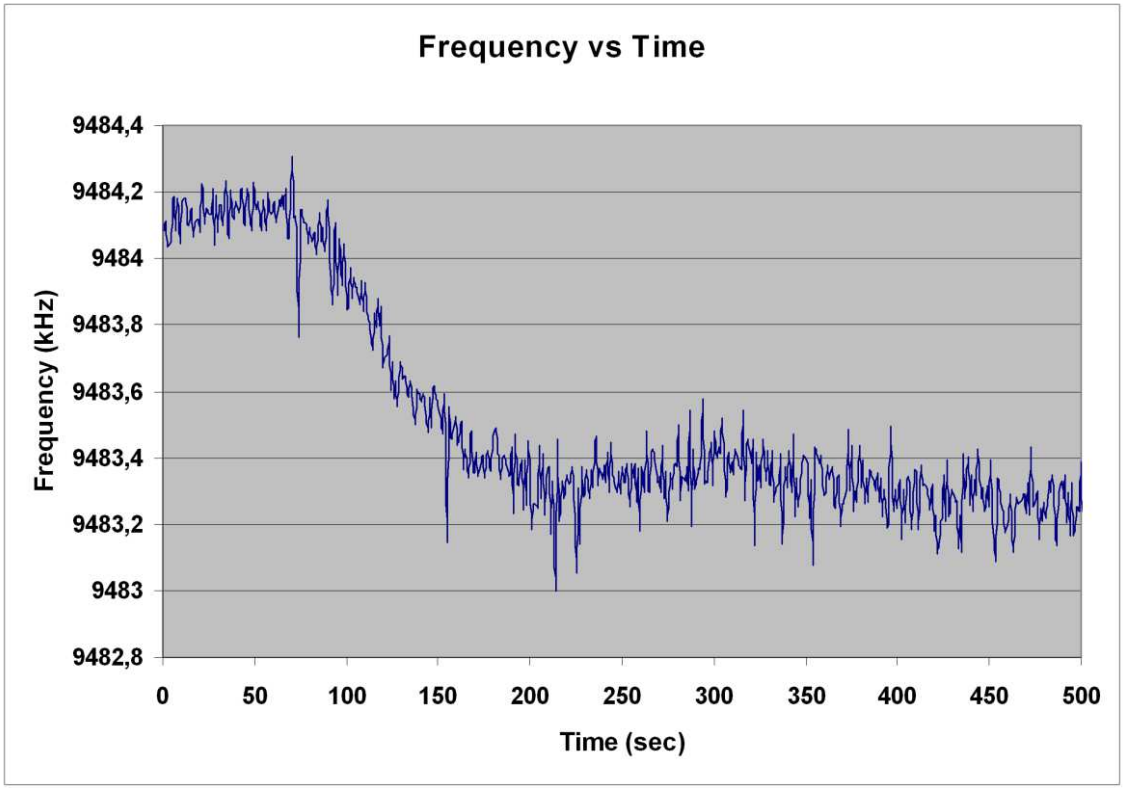
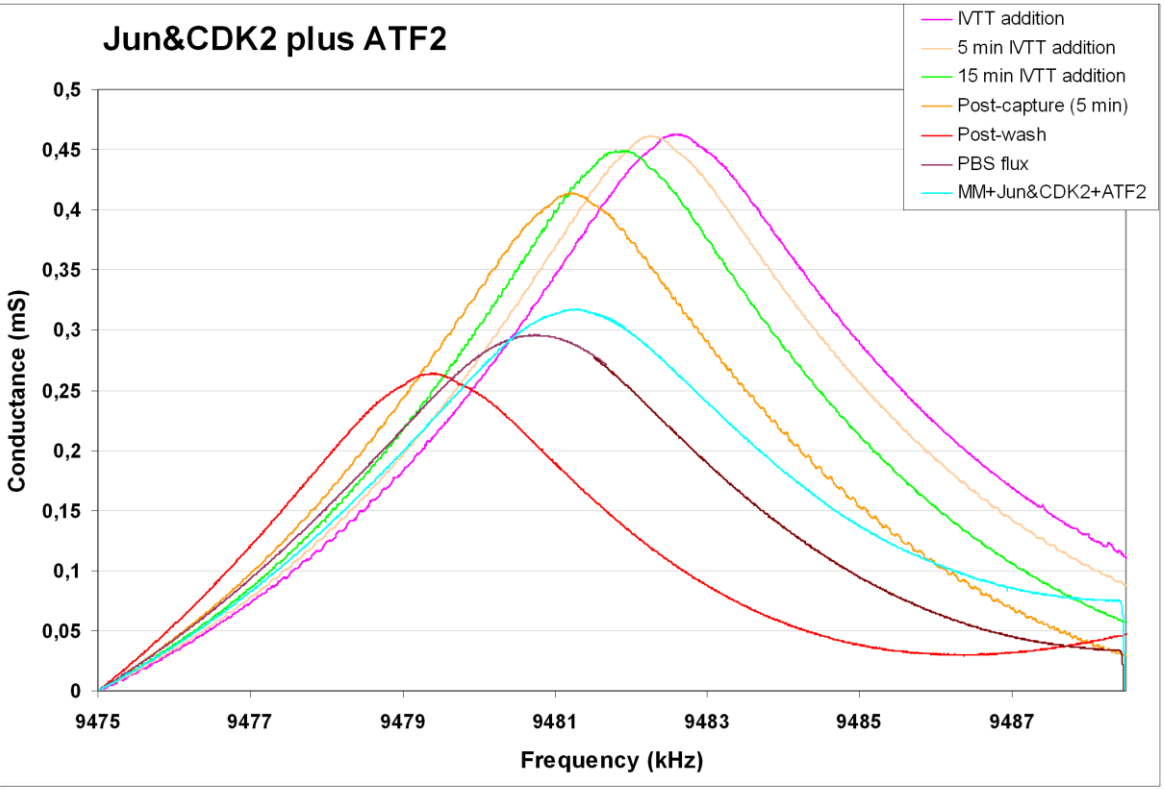

Frequency vs Time
Frequency (kHz)
9484,4
9484,2
9484
9483,8
9483,6
9483,4
9483,2
9483
9482,8
0
50
100
150
200
250
300
350
400
450
500
Time (sec)

Figure5:


Jun&CDK2 plus ATF2
IVTT addition
5 min IVTT addition
15 min IVTT addition
Post-capture (5 min)
Post-wash
PBS flux
MM+Jun&CDK2+ATF2
Conductance (mS)
0,5
0,45
0,4
0,35
0,3
0,25
0,2
0,15
0,1
0,05
0
9475
9477
9479
9481
9483
9485
9487
Frequency (kHz)

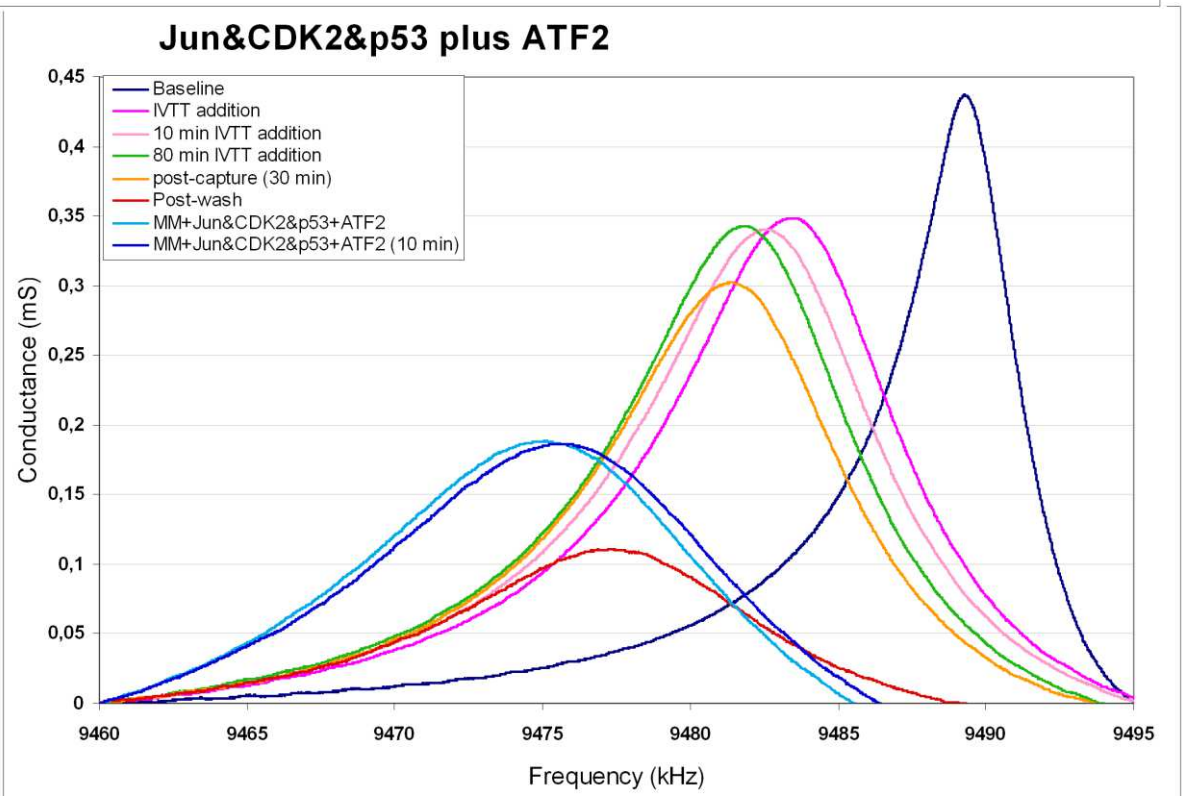

Jun&CDK2&p53 plus ATF2
Baseline
IVTT addition
10 min IVTT addition
80 min IVTT addition
post-capture (30 min)
Post-wash
MM+Jun&CDK2&p53+ATF2
MM+Jun&CDK2&p53+ATF2 (10 min)
Conductance (mS)
0,45
0,4
0,35
0,3
0,25
0,2
0,15
0,1
0,05
0
9460
9465
9470
9475
9480
9485
9490
9495
Frequency (kHz)

Figure 6:

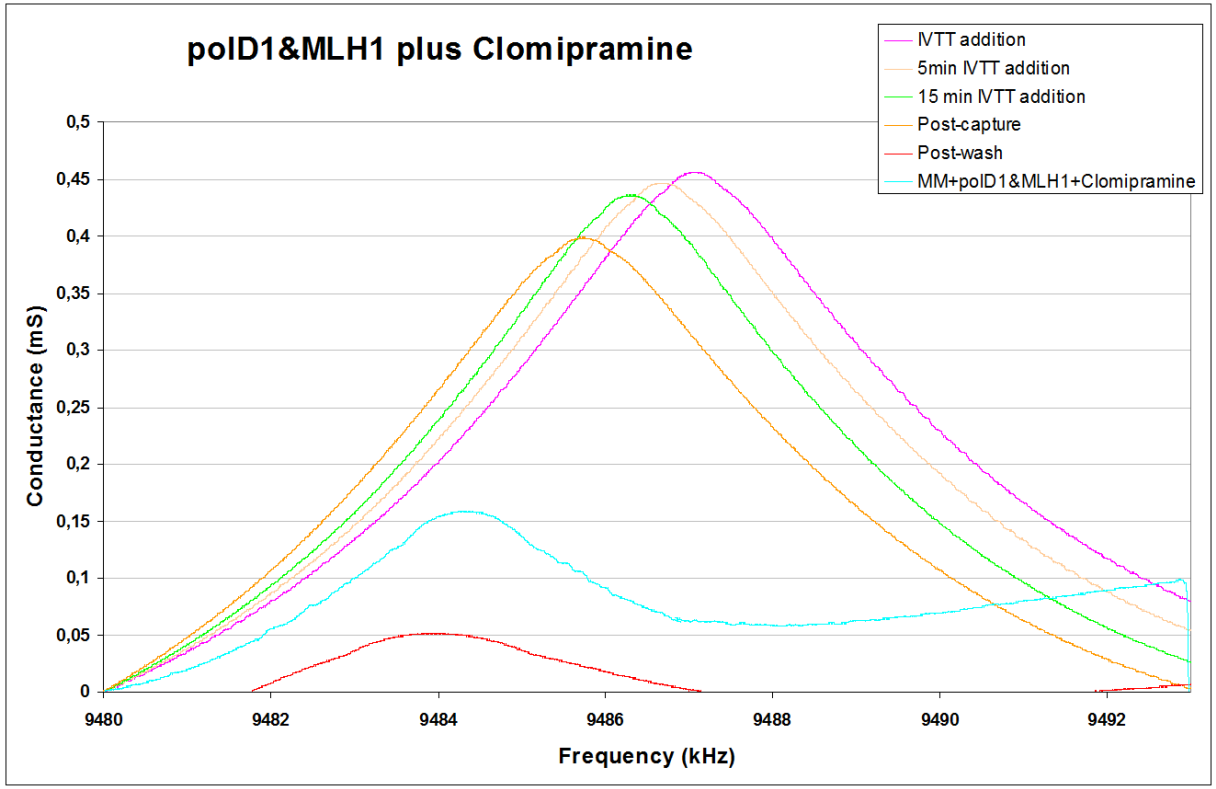

polD1&MLH1 plus Clomipramine
IVTT addition
5min IVTT addition
15 min IVTT addition
Post-capture
Post-wash
MM+polD1&MLH1+Clomipramine
Conductance (mS)
0,5
0,45
0,4
0,35
0,3
0,25
0,2
0,15
0,1
0,05
0
9480
9482
9484
9486
9488
9490
9492
Frequency (kHz)

Figure 7

Figure 2: Static Analysis for MM+BRIP1.
Steps are of 1 Hertz.

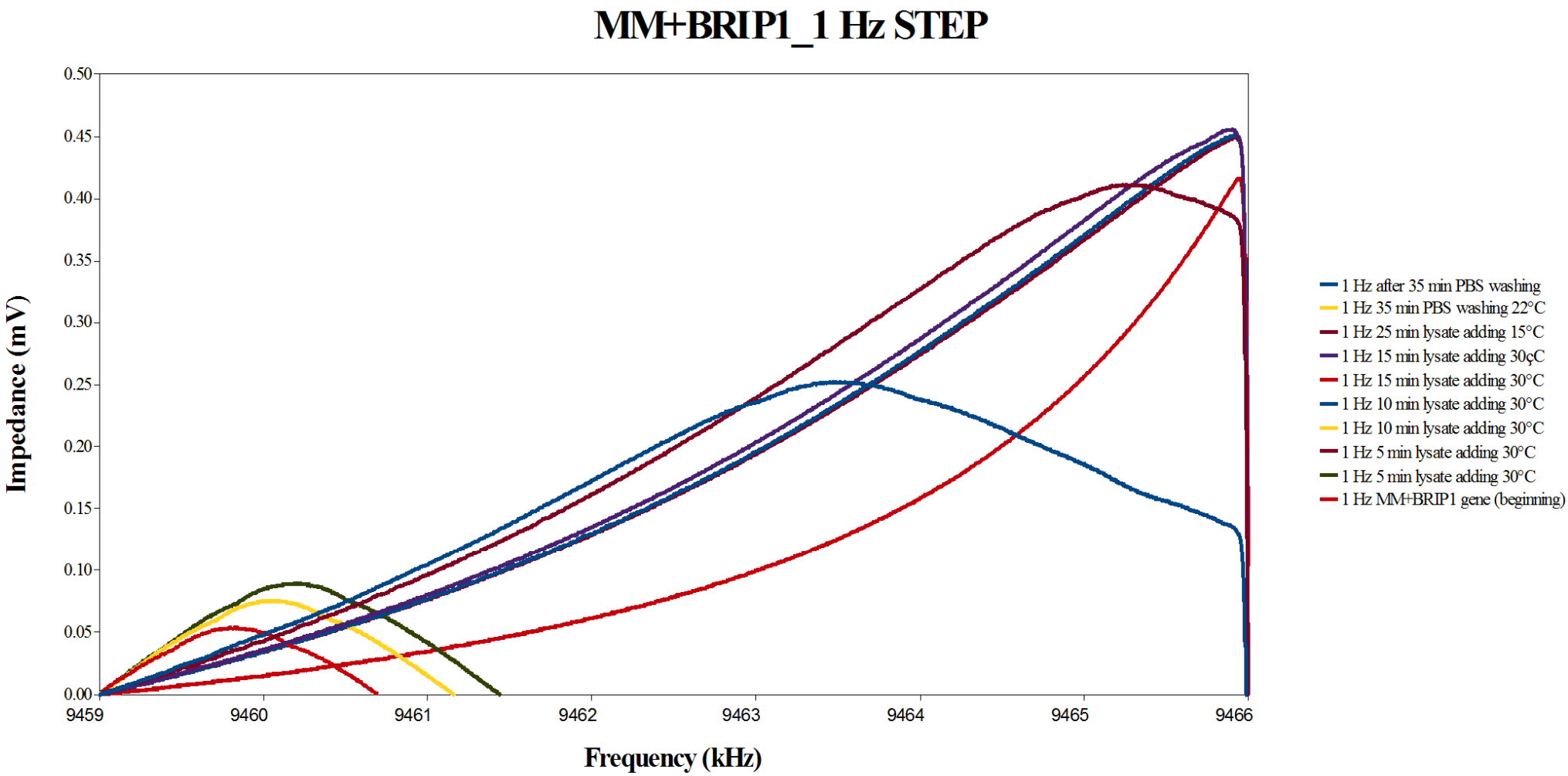


Figure 3: Static Analysis for MM+Jun plus ATF2.
Steps are of 6 Hertz.

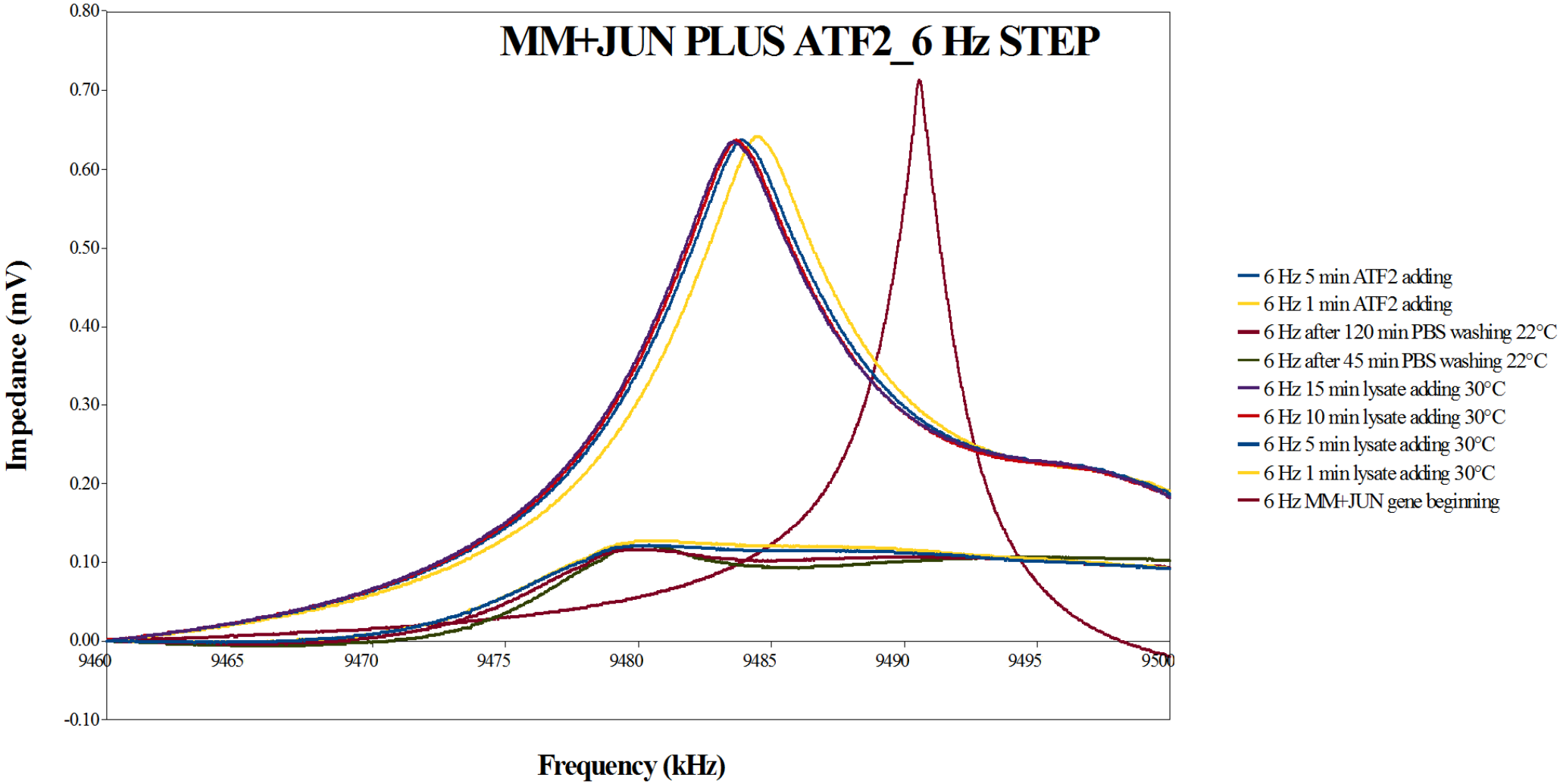
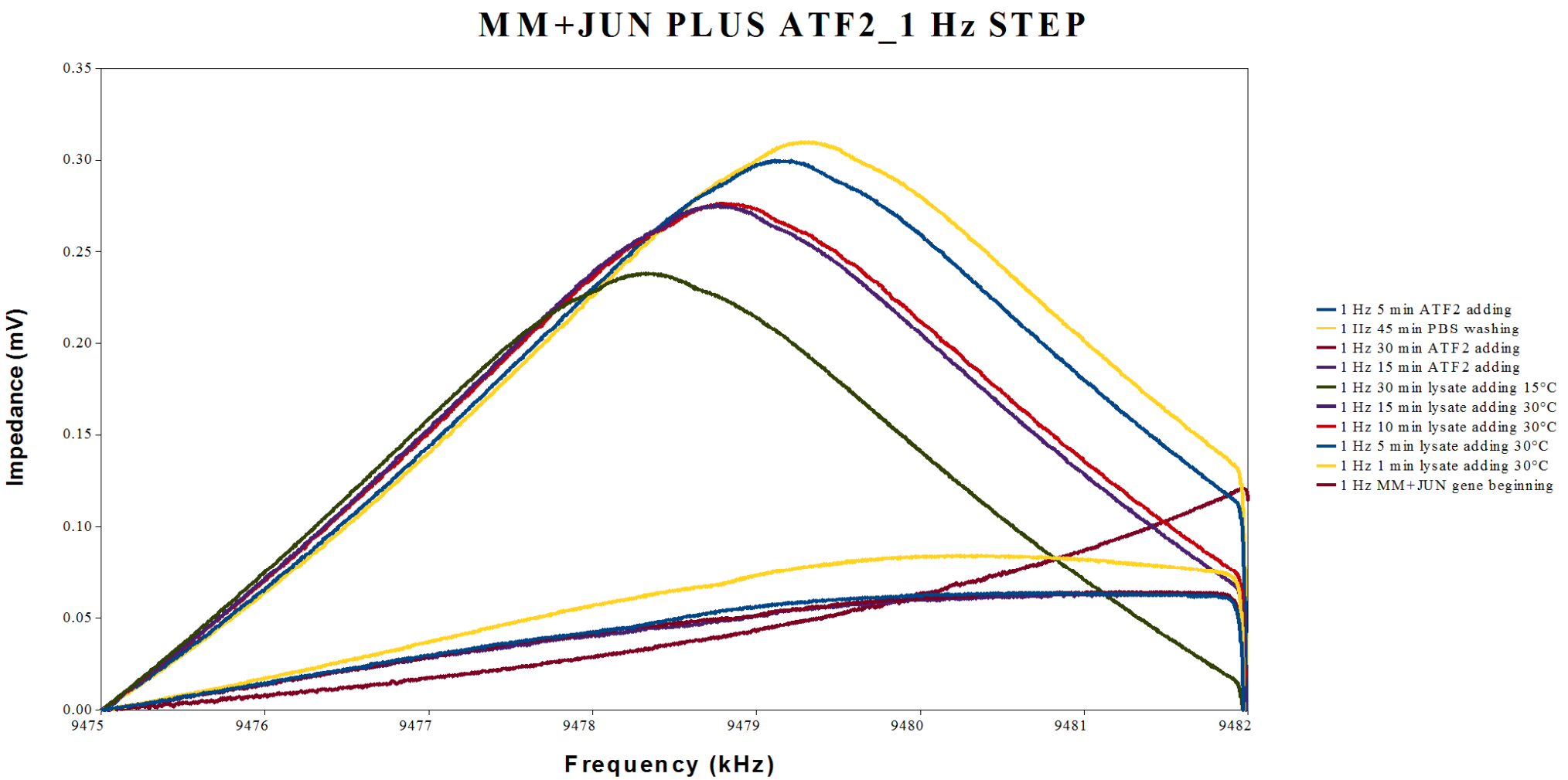
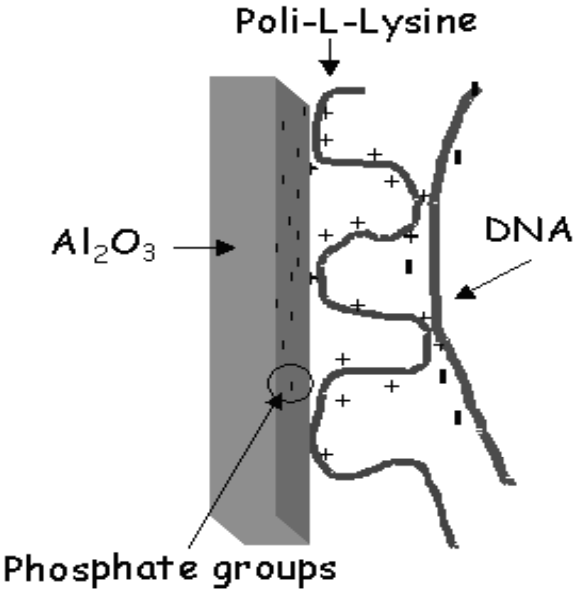
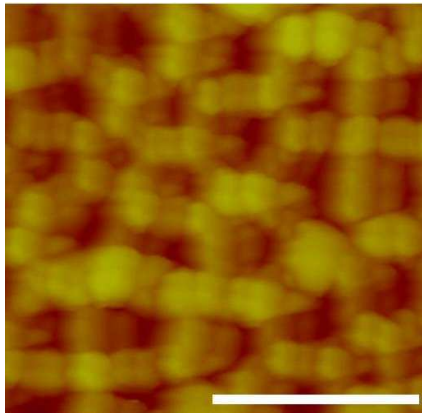


Figure 4: Static Analysis for MM+Jun plus ATF2.
Steps are of 1 Hertz.







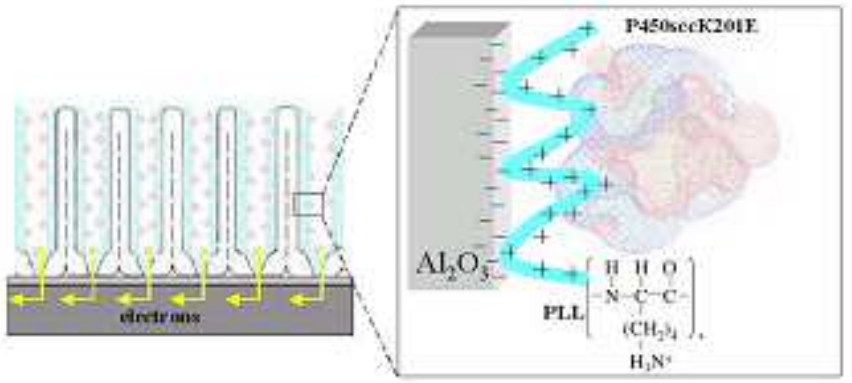
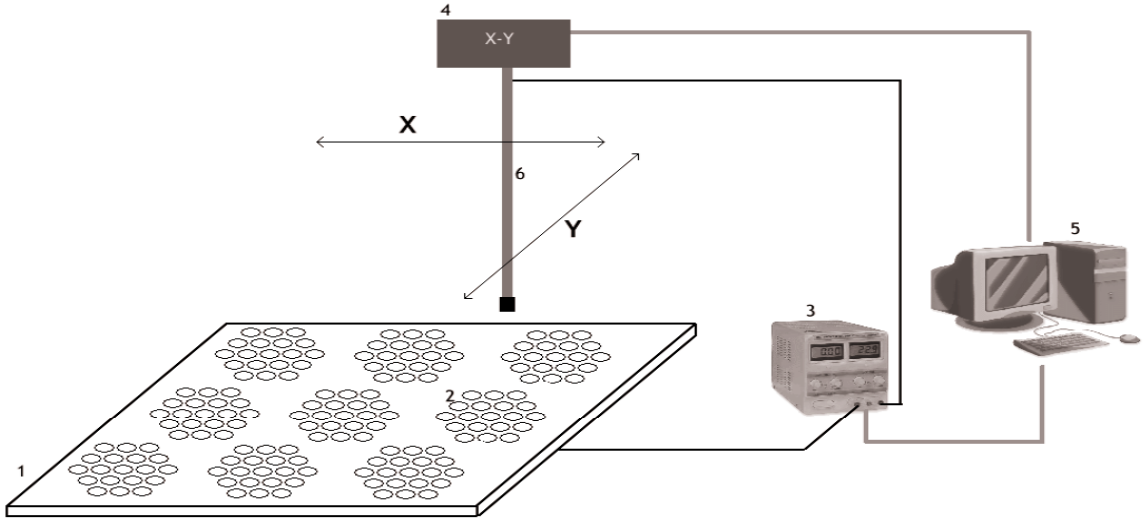


Figure 7. AFM images of cross-sectional morphologies of the APA microarray spot, resulting at the end of photolithographic microstructuring technique and 2 step anodization process. (center) and schemes of DNA-APA linkage via Poly-L-Lysine for genes microarray (left) and P450scc -APA linkage via Poly-L-Lysine for genes microarray for proteins microarray (right)

Figure 8

(left) Set up to analyze NAPPA elements using impedentiometric measurements: 1 – Aluminum substrate, serving also as counter electrode. 2 – APA spot, obtained by lithography, with biomolecules bound 3 – AC signal generator, controlled by PC. 4 – XY bidimensional actuator, controlled by PC, positioning the scanning electrode upon spots. 5 – PC, controlling bidimensional mover and AC signal generator. 6 – Scanning electrode, dipped in the solution containing NAPPA and buffer;

(right) Impedance spectroscopy plots in two spots of APA surface, one with protein hybridized to the probe molecule and another with probe only. Frequency ranges from 1 Hz to 100 KHz, voltage applied was 400 mVpp



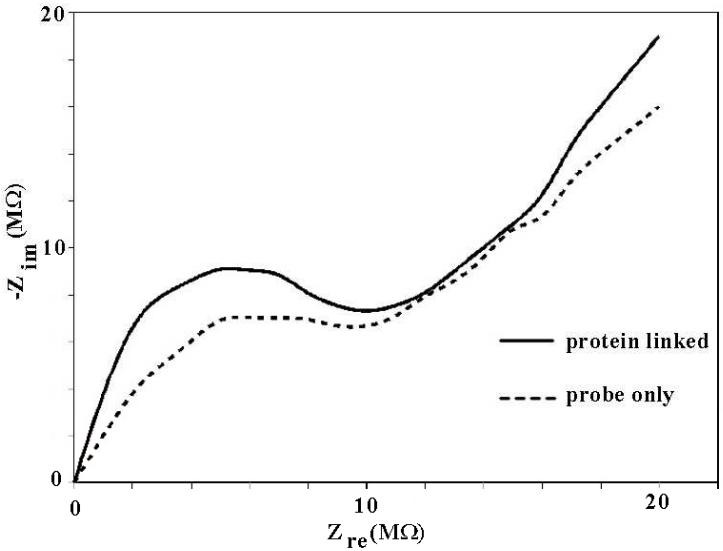


Figure 6.(Above) Single NAPPA fluorescence gene spot printed on APA after its expression in 2D (left) and in 3D (right). For comparison Atomic Force Microscopy of APA cross-section on glass in 2D is shown in the center. (Below , from left to right) To vary pore size and depth using Aluminum purity 99.999%, we vary from left ti right the acid concentration (0.5 M, 1M,1M) , the reaction time (150',30',120'), the voltage (30 V,30V,40V), the distance between two electrodes (1 cm., 2cm., 1cm).

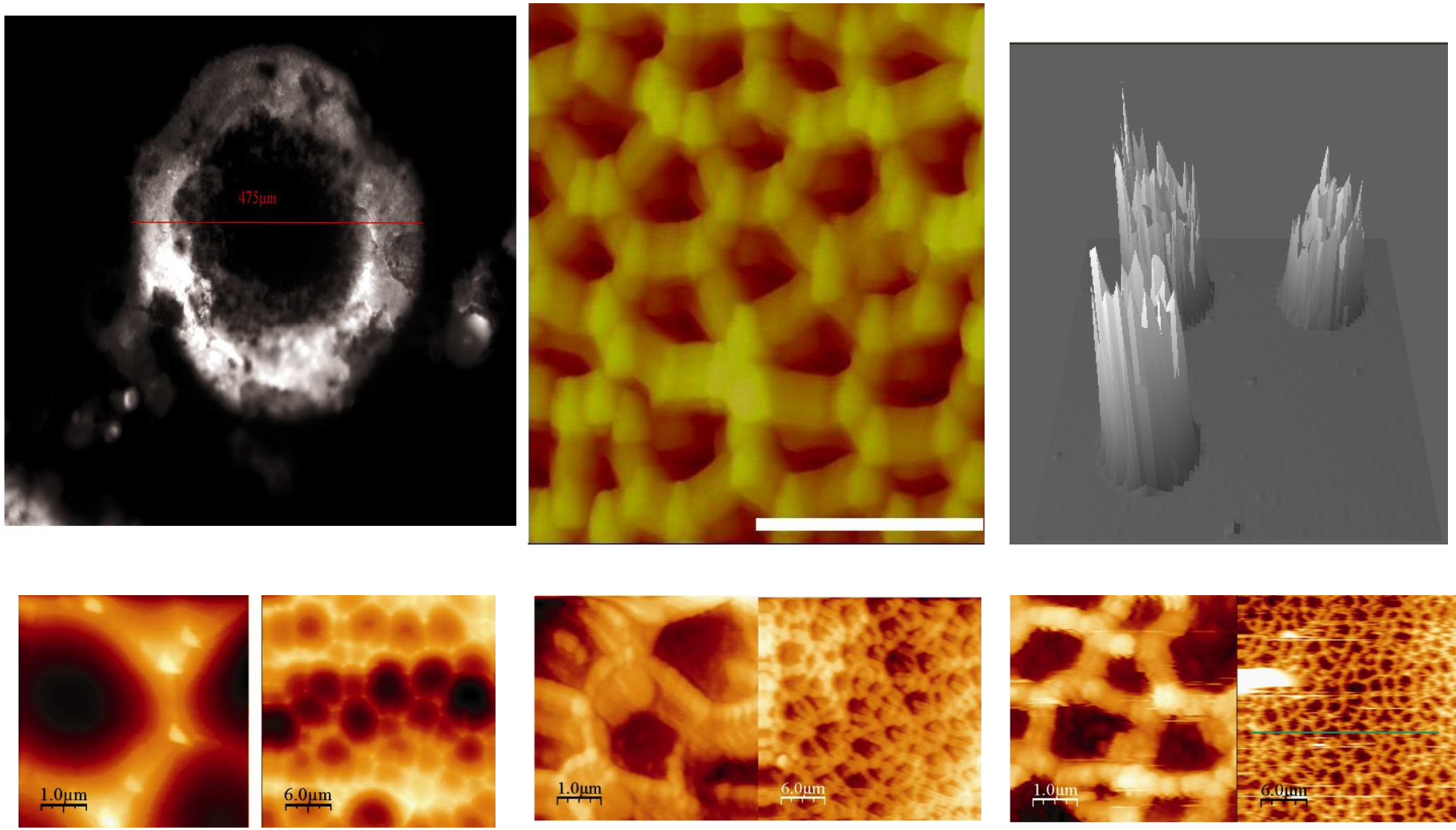


Figure 7 The future of APA is on the protein nanoarray printed using SNAP Genes based on bacterial cell free expression system (32) and pizoelectric inkjet technology (33); namely either for SNAP-APA nanoarray to evaluate protein-protein interactions in flow conditions , or for protein nanocrystallization where APA channels constitute very small wells for protein crystallization induced by LB monolayer of homologous proteins in presence of precipitate solution . The resulting patent is now pending submission (Table 1).

